Iowa State University

Department of Aerospace Engineering

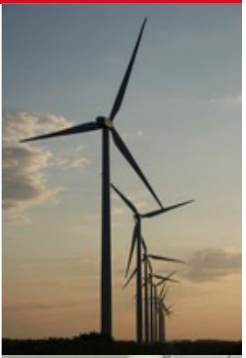

De-brief presentation: Fundamental Understanding of Pipeline Material Degradation under Interactive Threats of Dents and Corrosion

Ashraf Bastawros

Aerospace Engineering, Material Sciences and Engineering, Mechanical Engineering, Ames National Lab.

Vincent Holohan, TTI

Zhongquan Zhou, AOR,

Nusnin Akter, Program Manager

Office of Pipeline Safety-Engineering and Research Division

This material is based on work supported by the DOT-US Department of Transportation under Contract #693JK31950003CAAP, Project #838, and performed at Iowa State University

Iowa State University

Department of Aerospace Engineering

De-brief presentation: Fundamental Understanding of Pipeline Material Degradation under Interactive Threats of Dents and Corrosion

Kurt Hebert, Professor of Chemical Engineering, ISU

Kaustubh Kulkarni, Graduate Student (MS)

Amir Abdelmawla, Graduate Student (PhD)

Jessica Dwyer, Undergraduate Student (ME)

Kaiser Aguirre, Undergraduate Student (AerE)

Mehmet Sefer, Undergraduate Student (AerE)

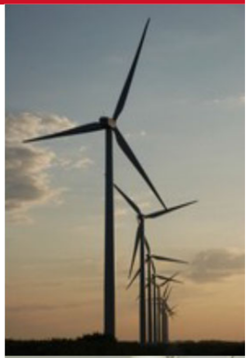

This material is based on work supported by the DOT-US Department of Transportation under Contract #693JK31950003CAAP, Project #838, and performed at Iowa State University

Mechanics and Materials

Ashraf Bastawros

Objective

Electrochemistry

Kurt Hebert

Enhance Pipeline Safety

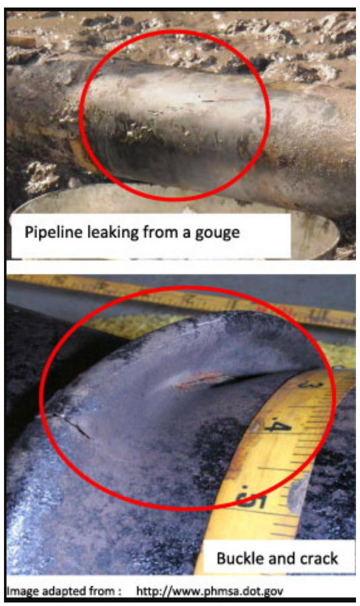

Evaluate interactive threats of external mechanical dents and secondary features, through integrated lab-scale experimental and numerical framework to characterize and better predict the remaining safe life and operating pressures, while projecting the needs for mitigation measures.

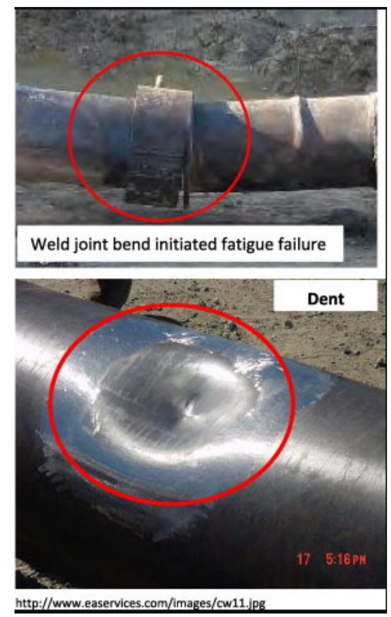

Pipeline failures in corrosive environments – A conceptual analysis of trends and effectshttps://doi.org/10.1016/j.engfailanal.2015.03.004

Motivation: Service Gauges and Dents

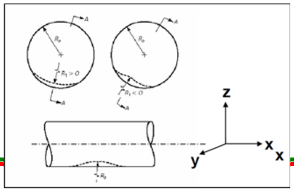

Figure 1 Picture of pipeline dent (Source: https://www.google.com/imghp?hl=en)

Failure Investigation Report – Northern Natural Gas Co (NNG) – Natural Force Damage

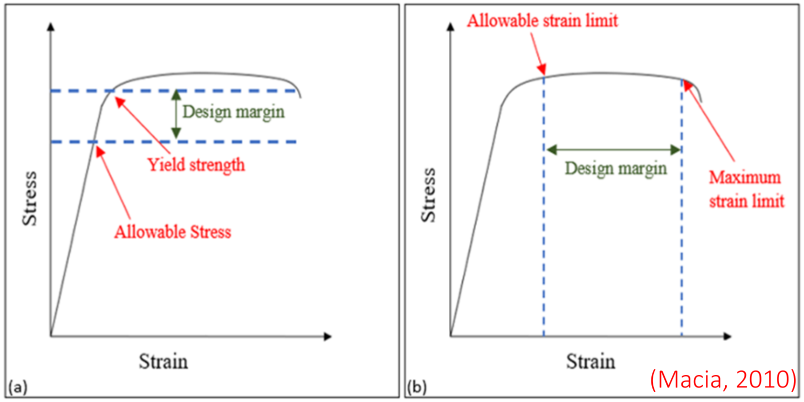

(a) Allowable stress-based design (b) Strain based design

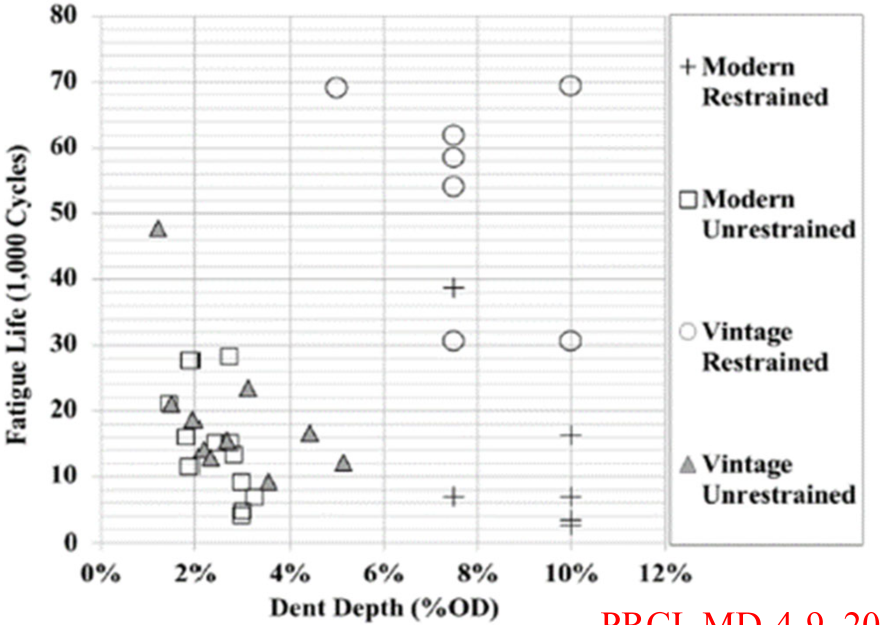

PRCI, MD-4-9, 2014

Large scatter of Fatigue Life vs. dent depth

Motivation: Interactive Threats

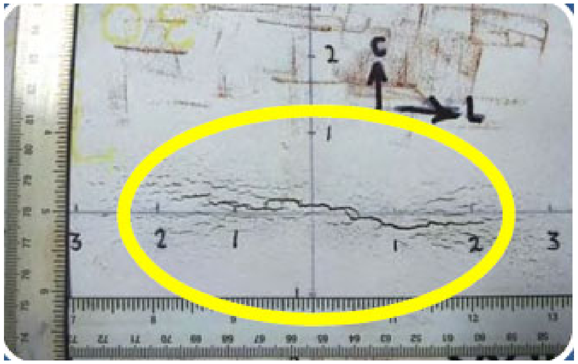

(a) Dented to 1.1% deep, unrestrained, fatigued (90-540psi), failed at 455k cycle.

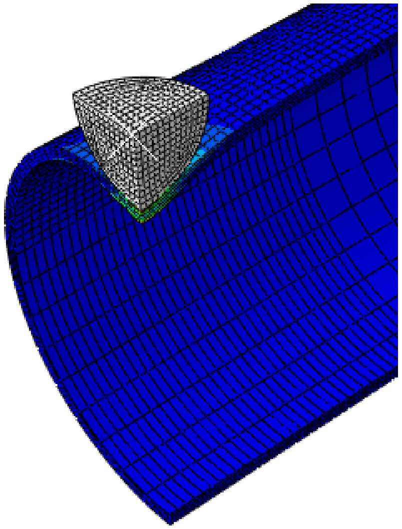

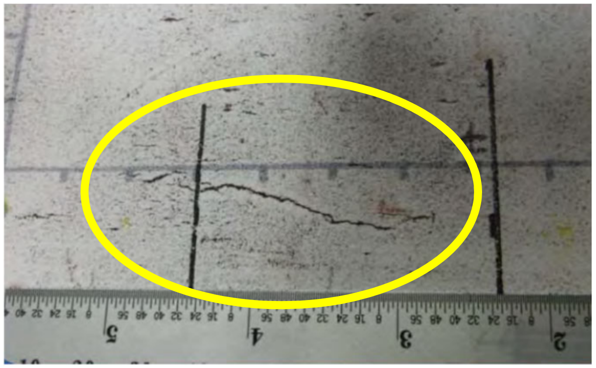

(b) In-service dent @1.6% deep, smooth profile, restrained/ unrestrained fatigued (90-365psi), failed at 108k cycle.

(c) In-service failure, dent @1.6% deep, very rough, corroded profile, restrained/ unrestrained, (365psi max), failed at 12k cycle.

Summary of Findings: Synergistic Interactions

Accumulated ε_p
Residual Stress
Geometric Effects

Pristine Pipeline (ε_p=0%) ~ 5 M-cycle

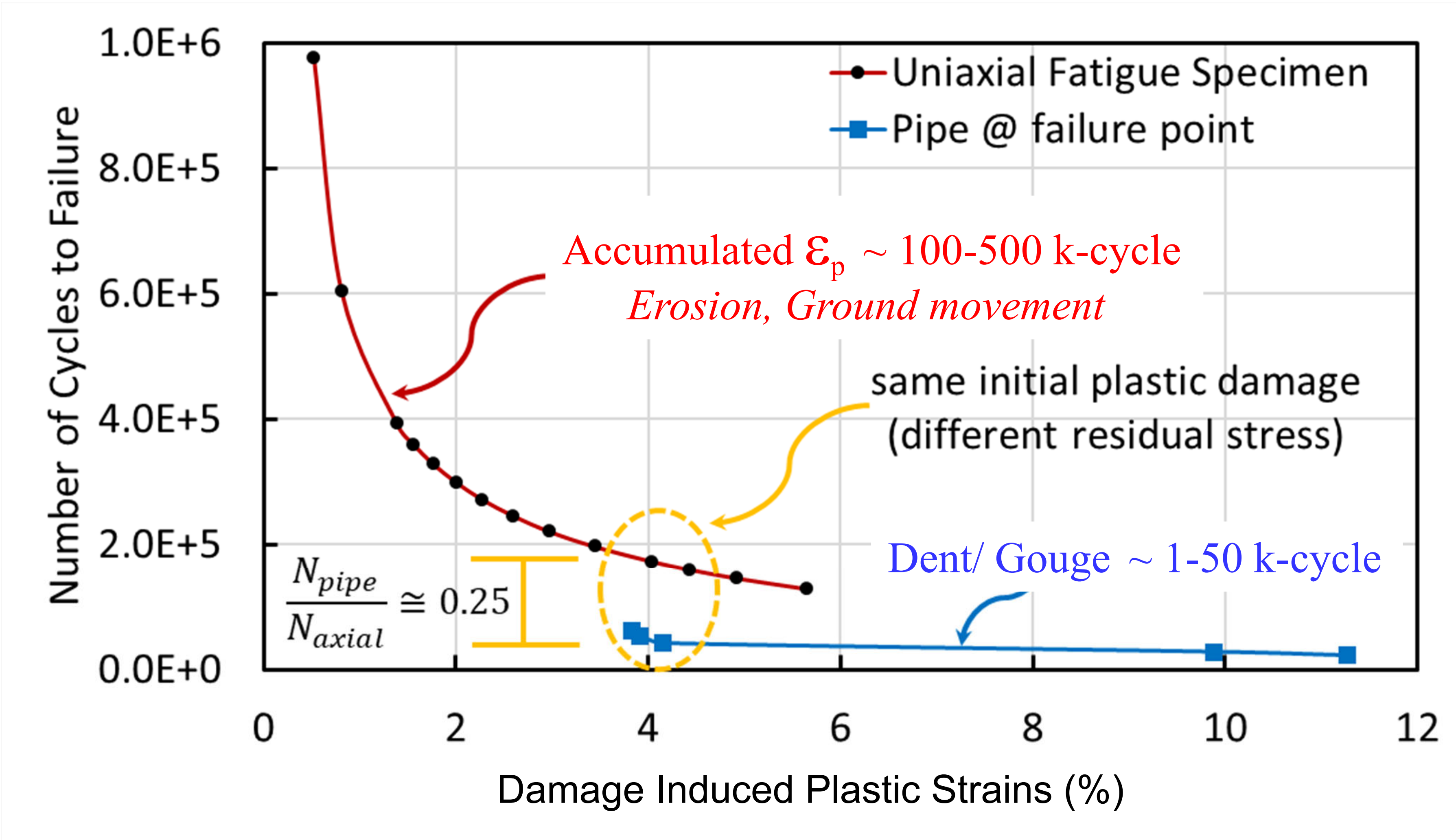

What could be the issue(s)?

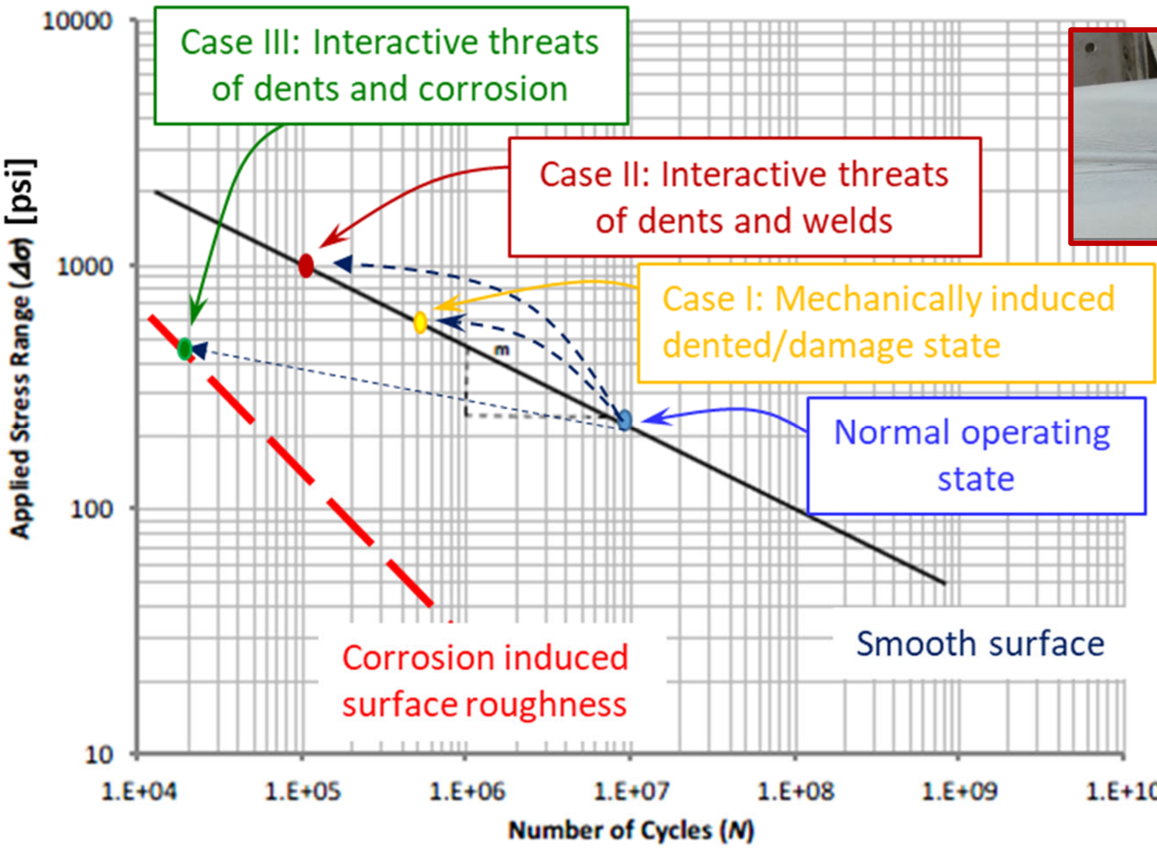

I. Initial Plastic Damage

II. Progressive Corrosion Damage

III. Interactive Chemo-mechanical Damage

Task-1: Lab Scale Interactive Threat Screening

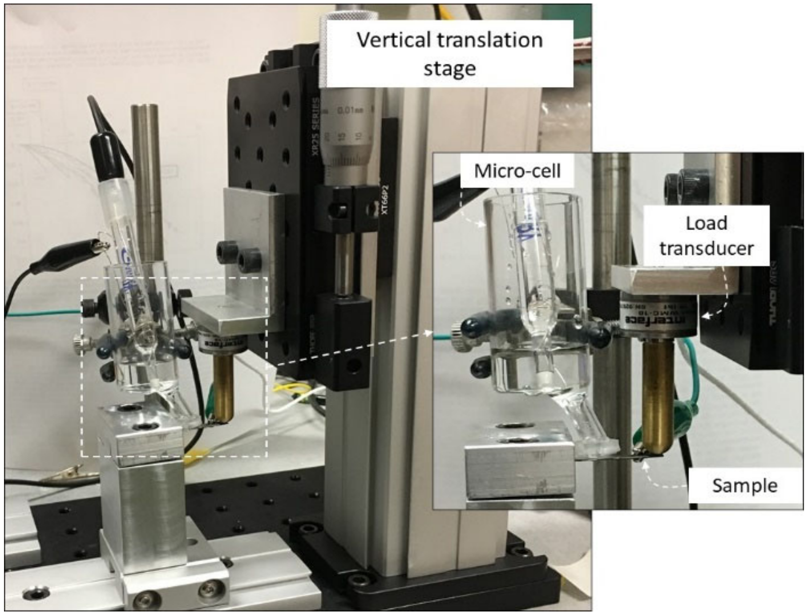

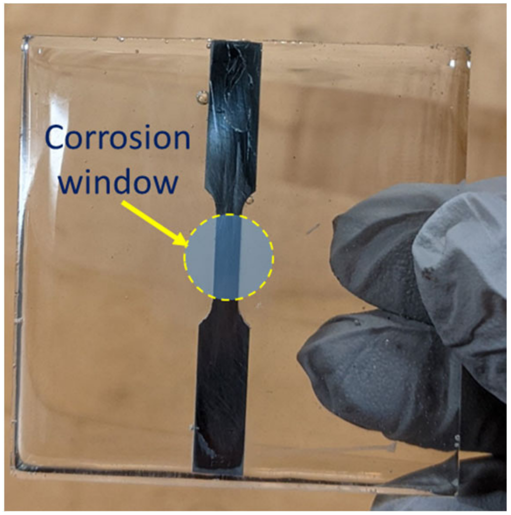

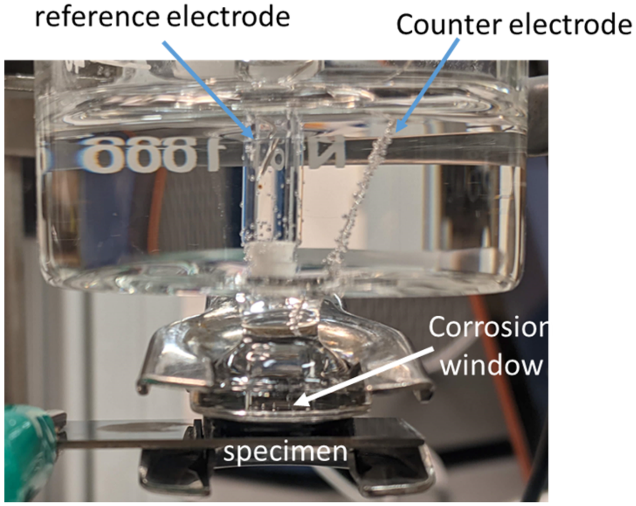

The micro-cell corrosion setup with the loading mechanism to mimic IGSCC conditions with variable stress levels.

Task-2: Electrochemical Effects: Experiments/electrochem. measurement

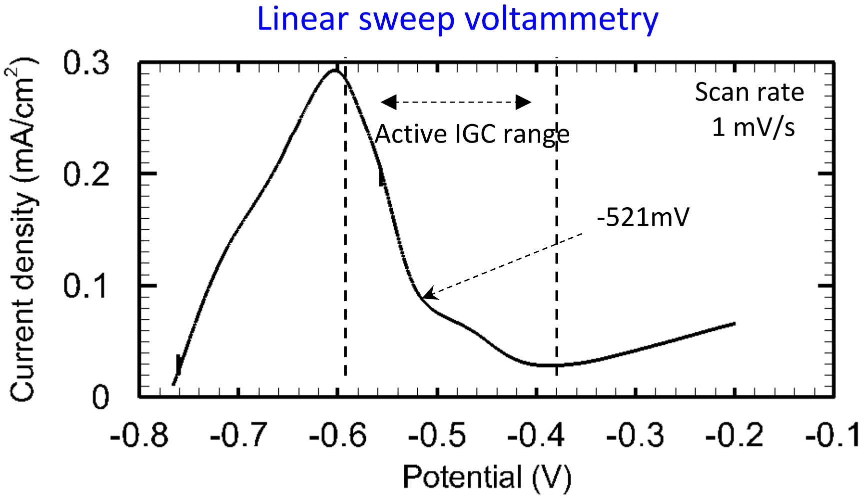

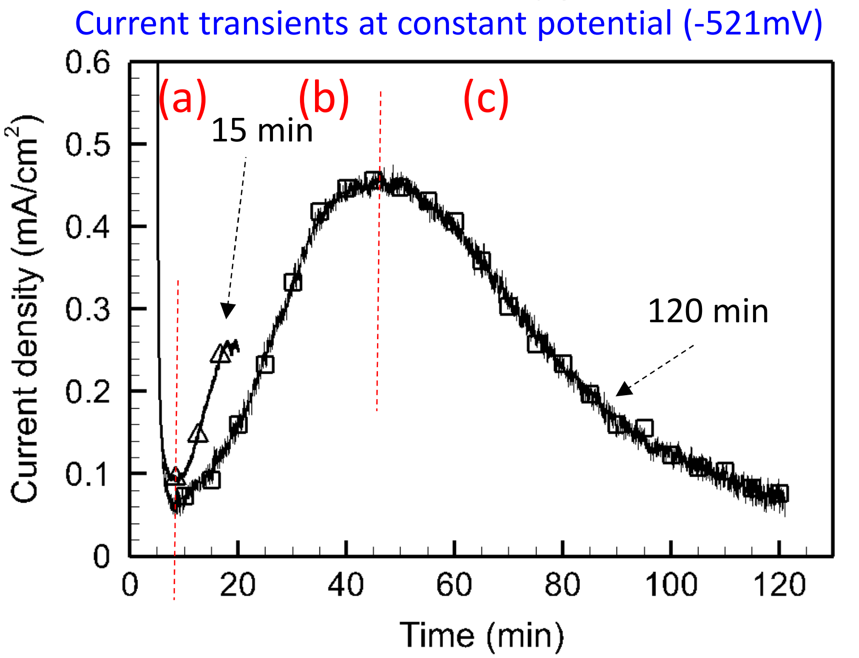

- Sodium bicarbonate solution at pH 8.2.
- Susceptible potential range for IGC (IGSCC) determined by linear sweep voltammetry.
- Potentiostatic experiments, there regimes in the current transients:
  - (a) Passivation of surface
  - (b) Metal dissolution & oxide formation
  - (c) Thickening of corrosion product layer

Surface morphology after potentiostatic experiments

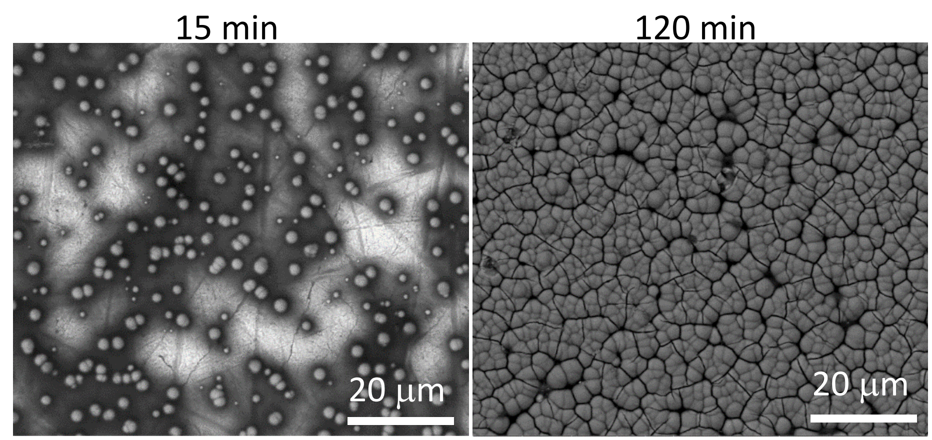

Task-2.1 Electrochemical Effects: Role of Plastic Strains

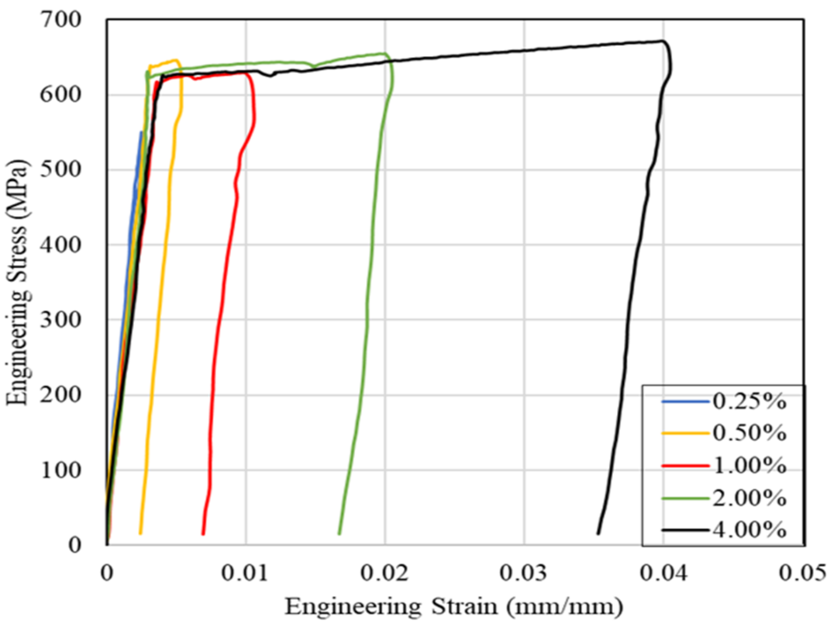

Loading to predetermined strain levels of 0.25-4%, representing the residual plastic strain level within a shallow dent.

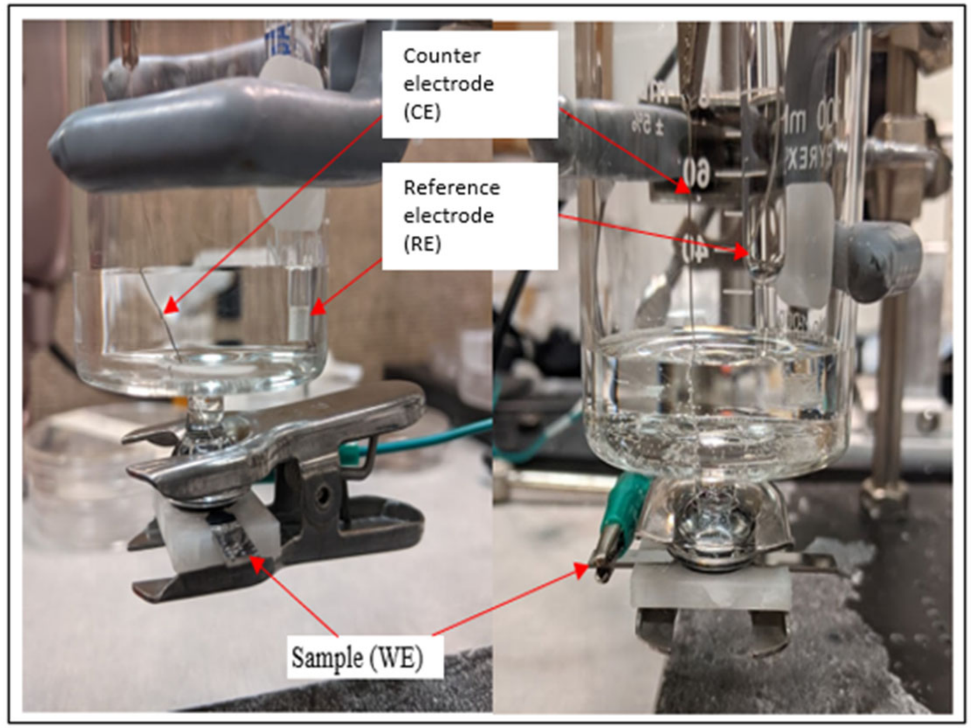

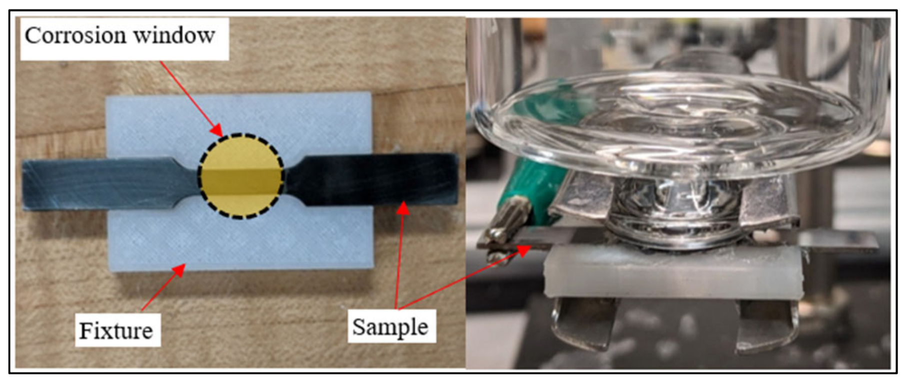

Coupled Chemo-mechanical corrosion (5hrs)

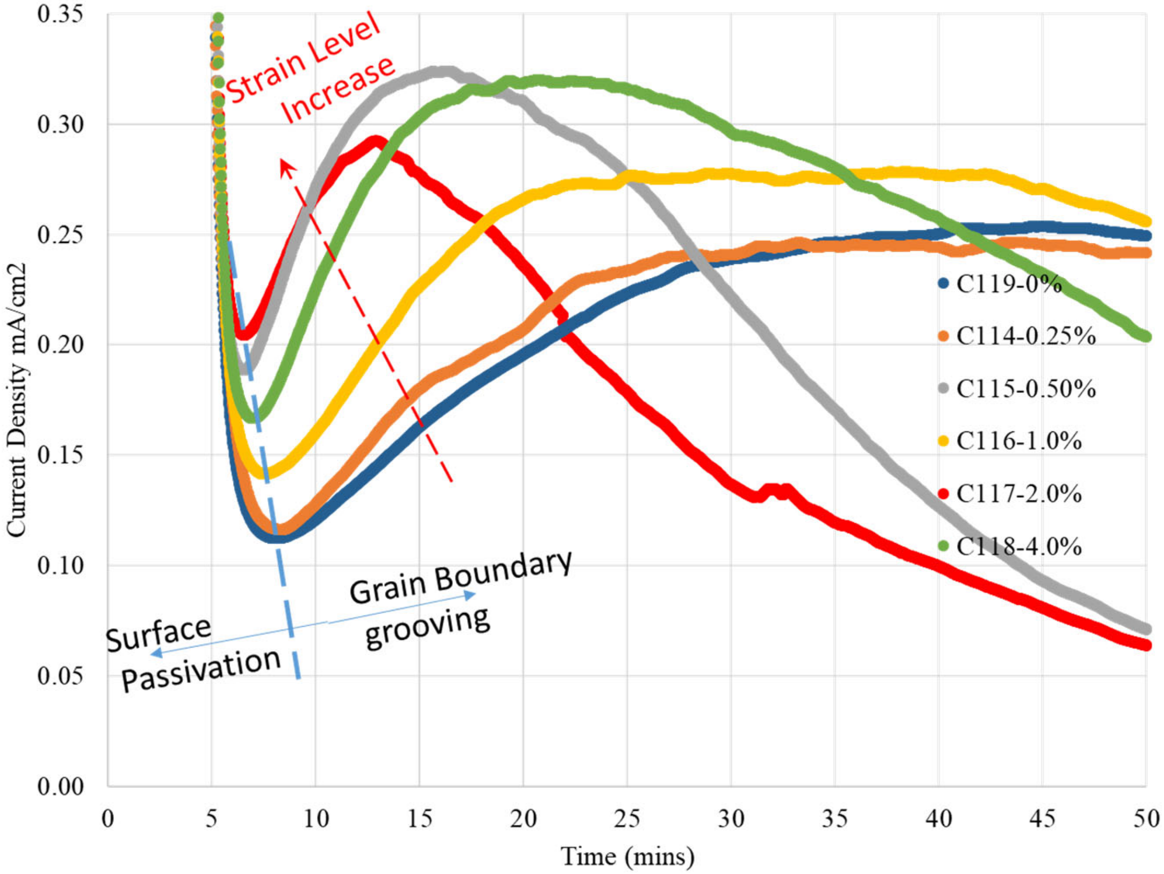

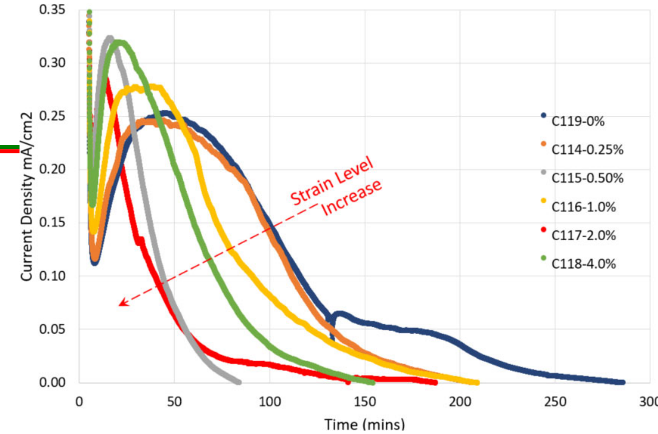

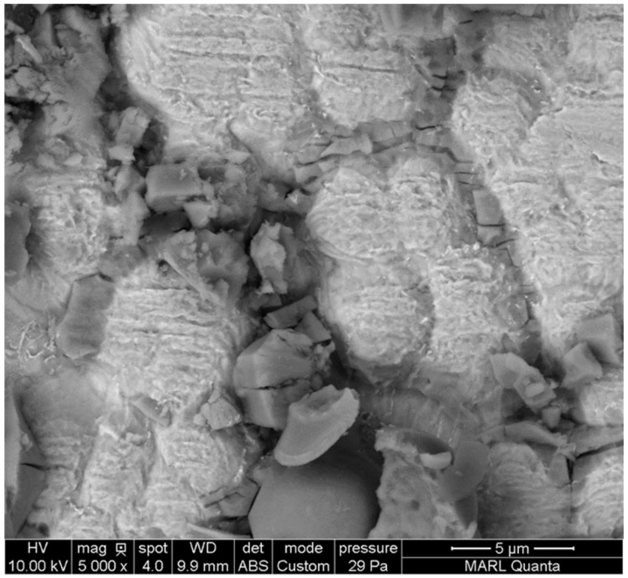

Corrosion at triple junction & GB
(5hrs, 0 % pre strained)

Coupled Chemo-mechanical corrosion (15min)

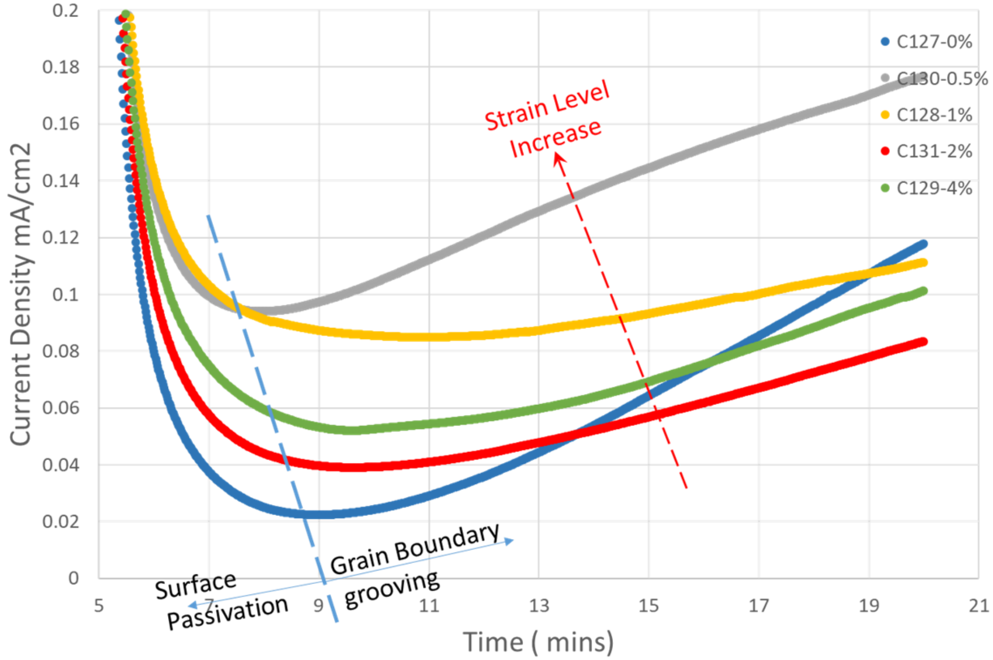

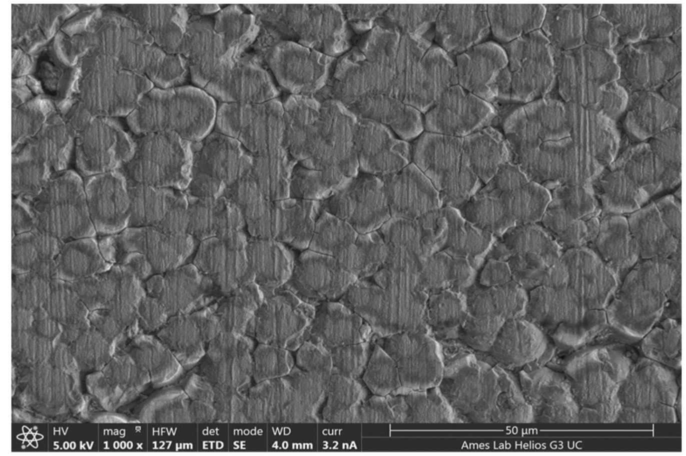

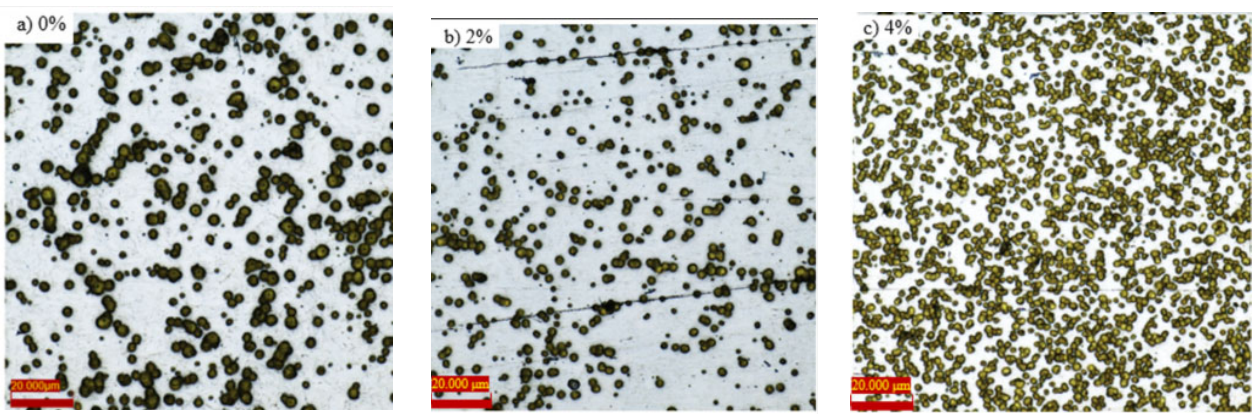

Strain Level Increase

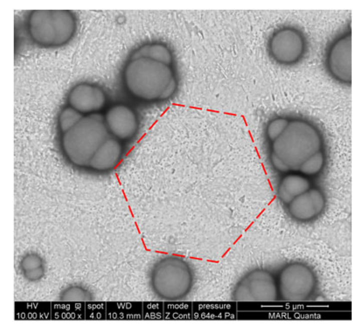

$$\% \text{ activation site} = \frac{\text{No active sites}}{N_{TJ}}$$

Variation of Activation Site Density with pre-Strain Level

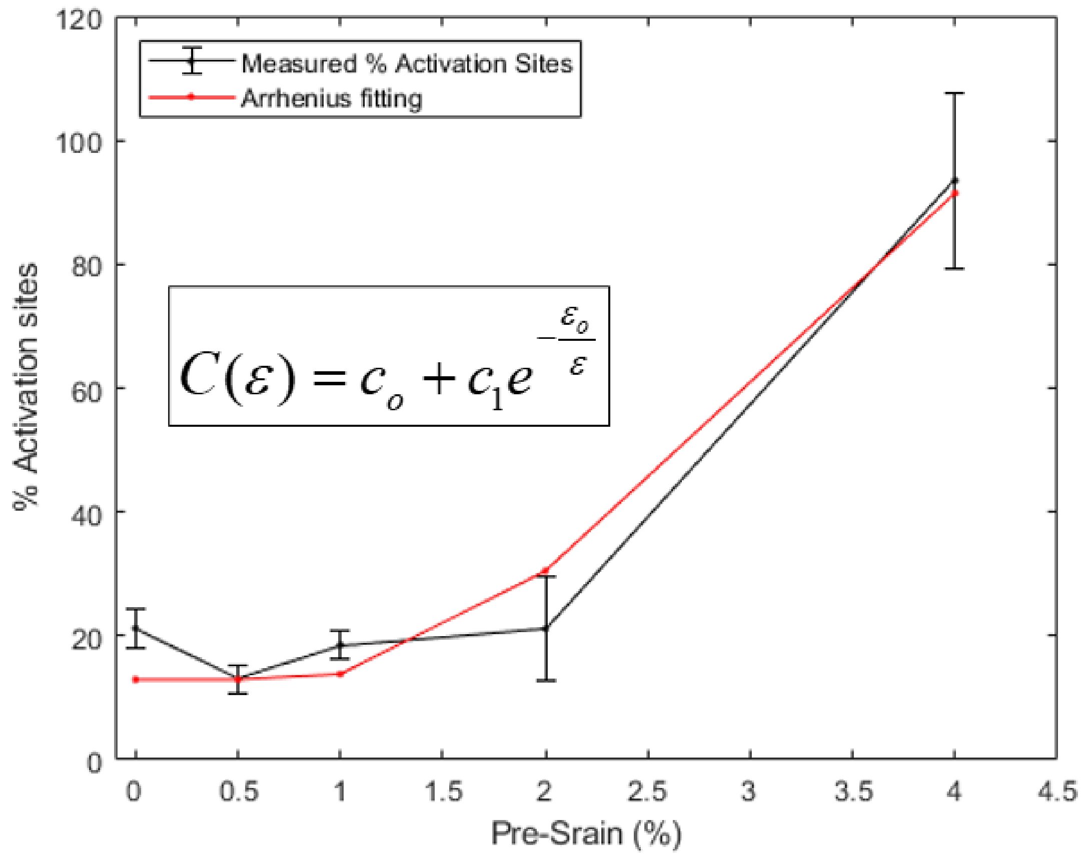

C(ε) is the percentage activation sites as a function of the prestrain level

C_o = reference site densities (0.13) ε_o = reference strain (0.06) C_1= const. (3.51)

Arrhenius dependence of density of the triple junction corrosion site on the strain level.

(3.1) EIS Analysis: Corrosion Product Layer

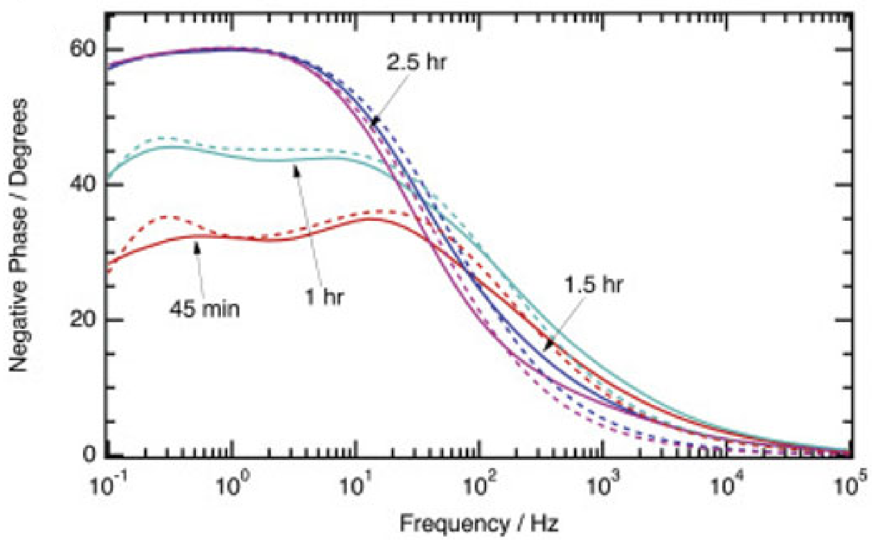

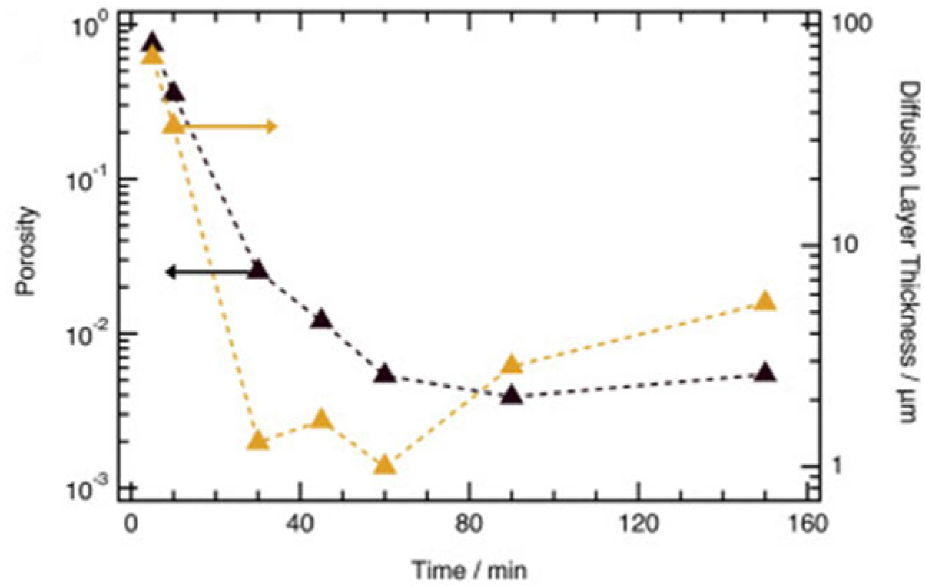

Dependence on corrosion time of porosity φ and diffusion layer thickness δ

Task-3.2 Electrochemical Analysis: (a) Grain Boundary Grooving

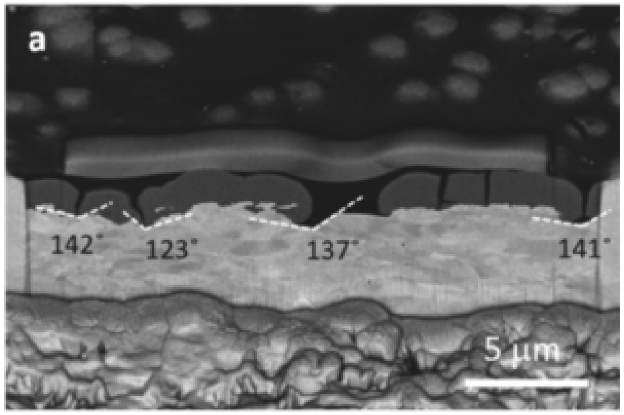

2hrs exposure

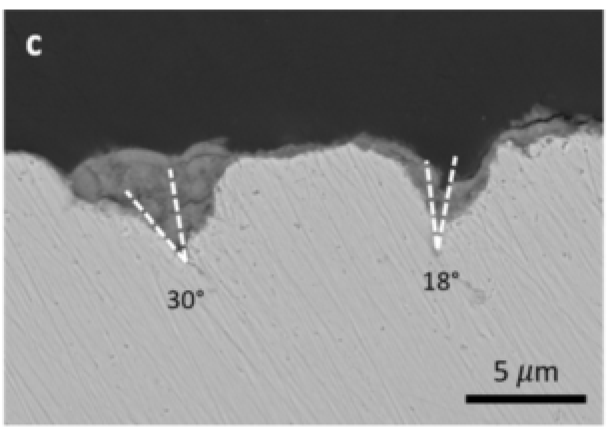

5hrs exposure

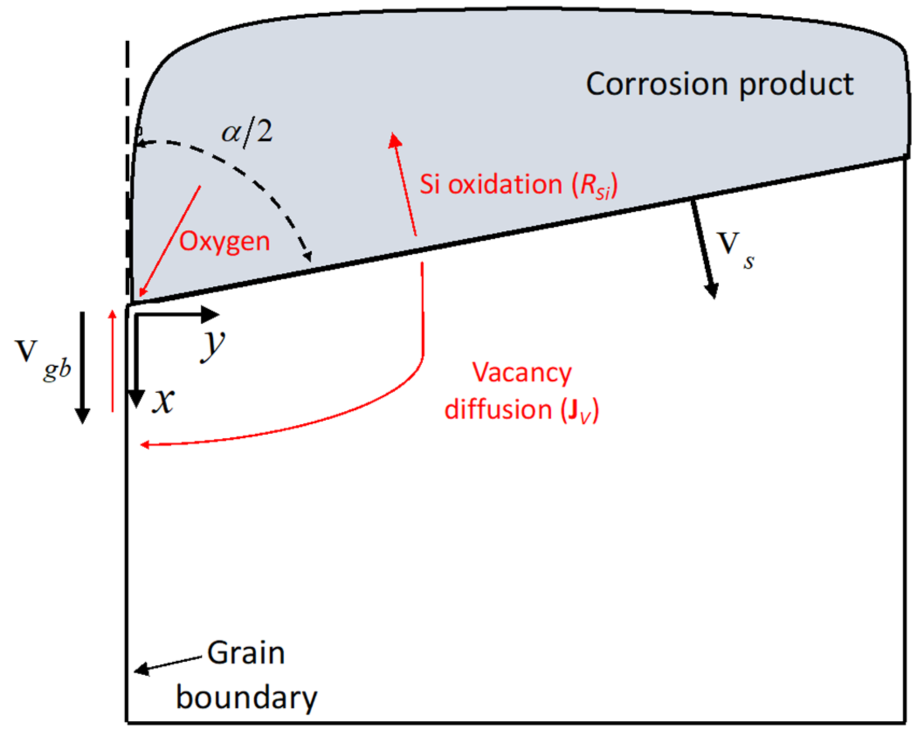

Solving diffusion eqn. by multigrid finite difference

- Shape evolution
- Vacancy Concentration

Misra et al. 2021

Task-3.2 Electrochemical Analysis: (a) Grain Boundary Grooving

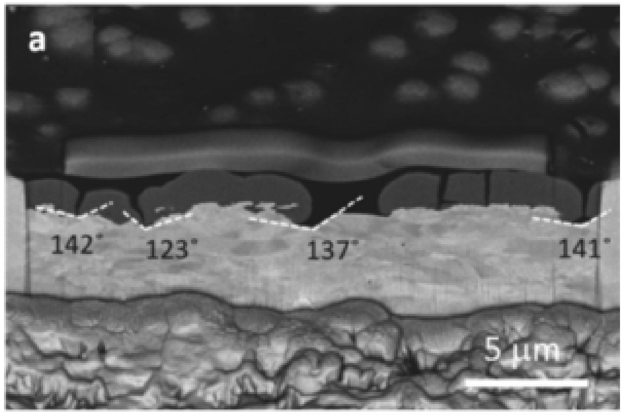

2hrs exposure

Vacancies concentration, c(x,y)

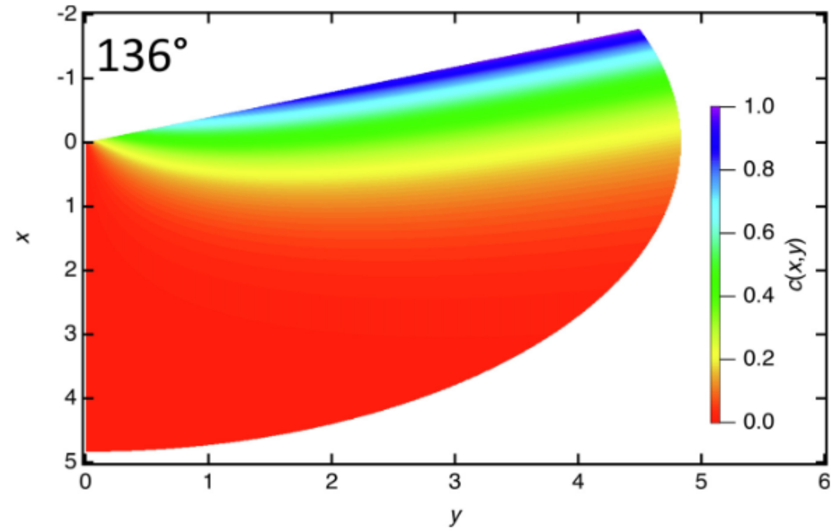

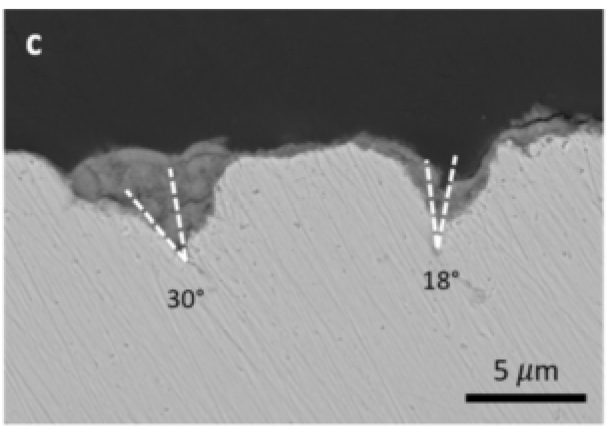

5hrs exposure

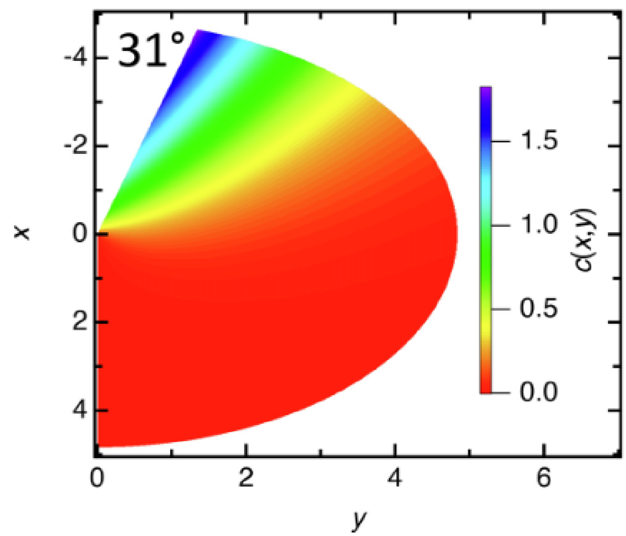

Misra et al. 2021

Task-3.2 Electrochemical Analysis: (b) Evolution of GB Cracking

5hrs exposure

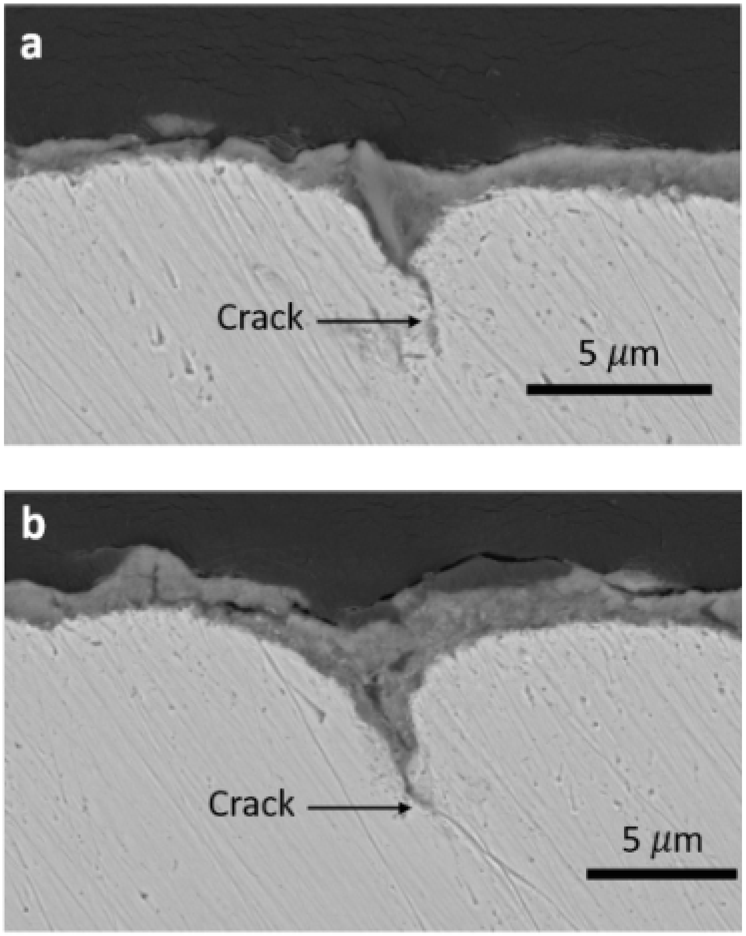

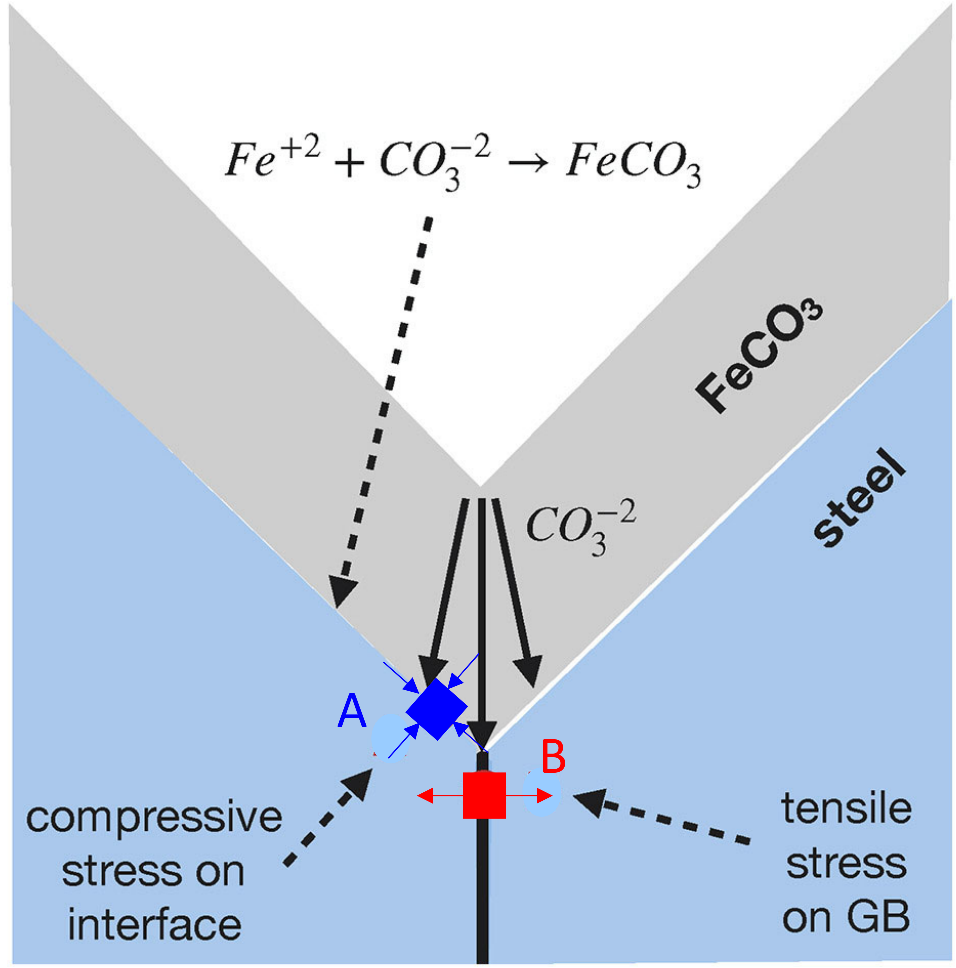

$FeCO_3$ corrosion product layer grows at the metal interface by inward diffusion of CO_3^{-2} ions.

Point A: volume expansion, compressive out-of-plane stress in the steel,

Point B: tensile stress concentration at the GB ahead of the wedge

Misra et al. 2020

Task-3.2 Electrochemical Analysis: (c) Fatigue Life

5hrs exposure

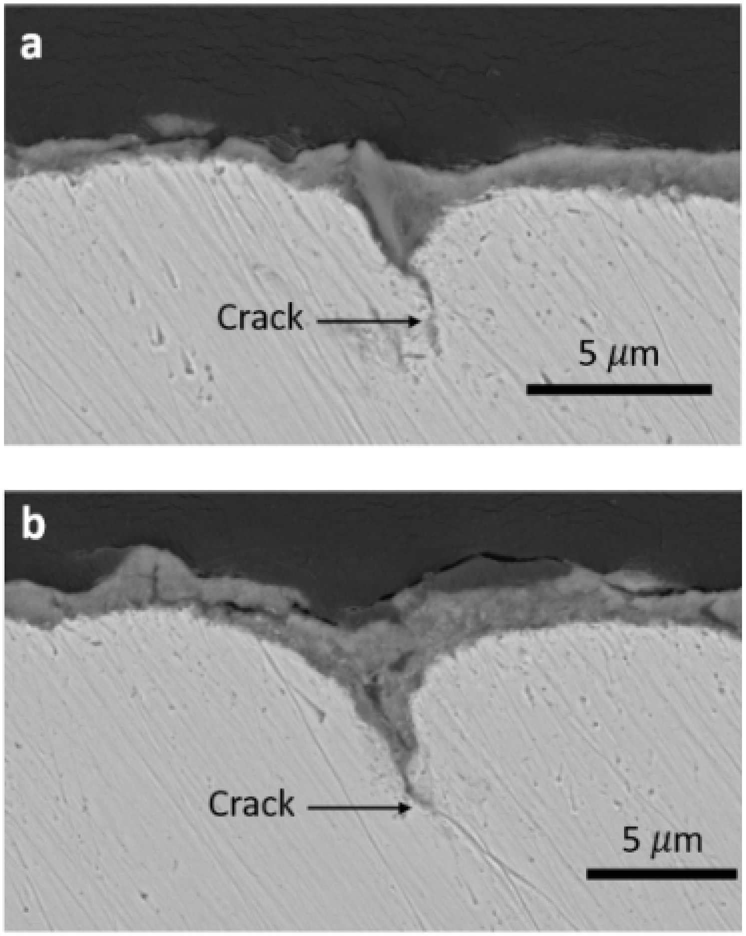

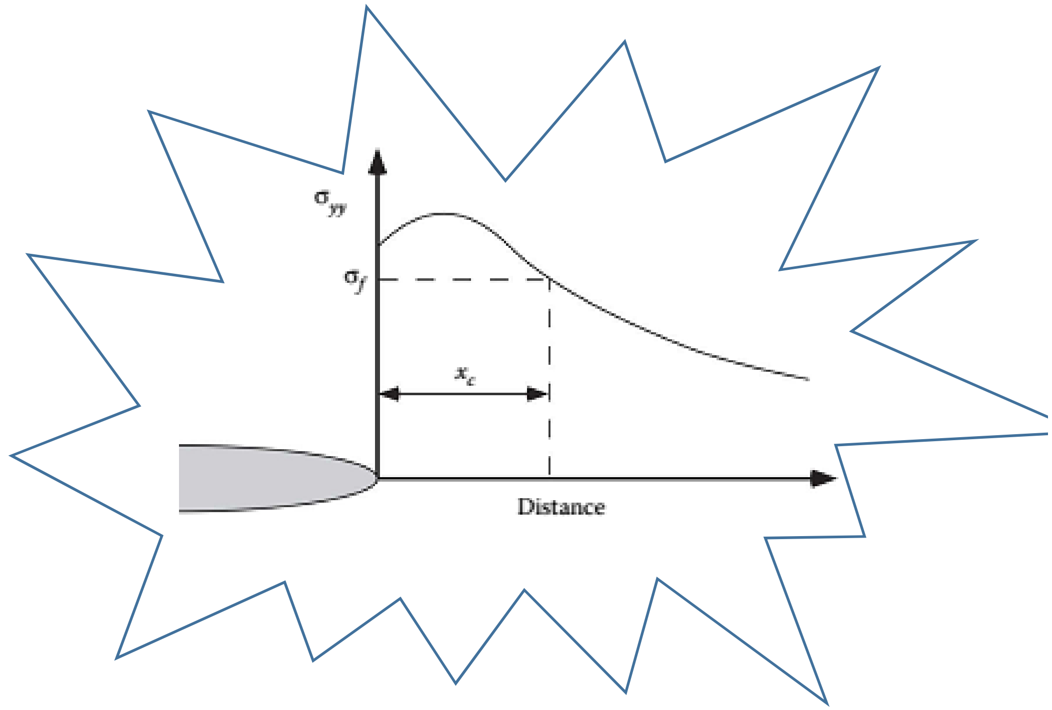

The RKR model for cleavage fracture.
(Ritchie, Knott, Rice, 1973.)

- Additional efforts required to couple electrochemical driven GB cracking to Fatigue life

Task-4: Numerical Analysis of Interactive Threats

Figure 1 Picture of pipeline dent (Source: https://www.google.com/imghp?hl=en)

(4.1) Elasto-plastic cyclic damage constitutive model

Framework proposed by LeMaitre and Chaboche

$$\epsilon_{ij}^{t} = \epsilon_{ij}^{e} + \epsilon_{ij}^{p}$$

$$\epsilon_{ij}^{e} = \frac{1+\nu}{E}\left(\frac{\sigma_{ij}}{1-D}\right) - \frac{\nu}{E}\left(\frac{\sigma_{kk}\delta_{ij}}{1-D}\right)$$

$$f_y = \sqrt{\frac{3}{2}\left(\frac{\sigma_{ij}}{1-D} - \alpha_{ij}\right)\left(\frac{\sigma_{ij}}{1-D} - \alpha_{ij}\right)} - R(\bar{\epsilon}_p)$$

$$\dot{\epsilon}_{ij}^{p} = \dot{\lambda}\left(\frac{\partial f_y}{\partial \sigma_{ij}}\right)$$

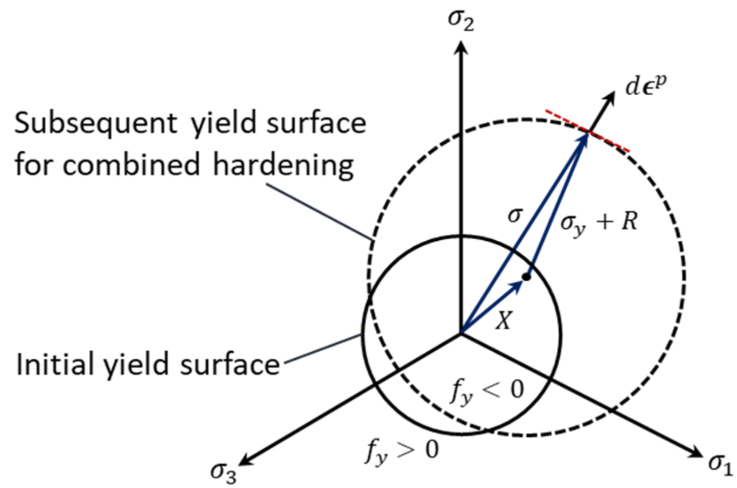

Accumulated damage per cycle block

$$\boxed{D^{i+1} = D^{i} + \left(\frac{dD_e}{dN} + \frac{dD_p}{dN}\right)\Delta N}$$

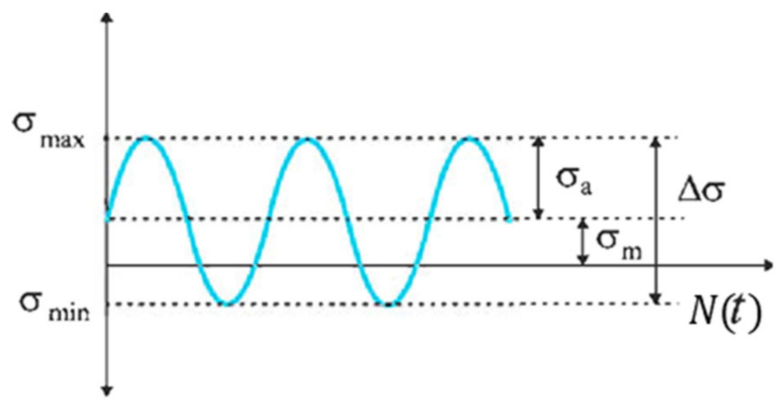

Task-4.2 Fatigue Damage Model

Elastic Damage Evolution

elastic damage per cycle

$$\boxed{\frac{dD_e}{dN} = [1-(1-D)^{\beta+1}]^{\alpha}\left[\frac{\tau_a}{M_o(1-3b_3\sigma_{H,mean})(1-D)}\right]^{\beta}}$$

$$\tau_a = \frac{1}{2}\left[\frac{3}{2}(S_{ij,max} - S_{ij,min})(S_{ij,max} - S_{ij,min})\right]^{1/2}$$

$$\alpha = 1 - a\left\langle\frac{\tau_a - \tau_a^*}{\sigma_u - \sigma_{eqv,max}}\right\rangle$$

$$\tau_a^* = \sigma_{lo}\left(1 - b_1(3\sigma_{H,mean}/\sigma_u)\right)$$

Plastic Damage Evolution

Lemaitre plastic damage formula

$$\boxed{\frac{dD^p}{dN} = \left[\frac{(\sigma_{eq})^2 R_v}{2ES(1-D)^2}\right]^m \Delta\bar{\epsilon}_p}$$

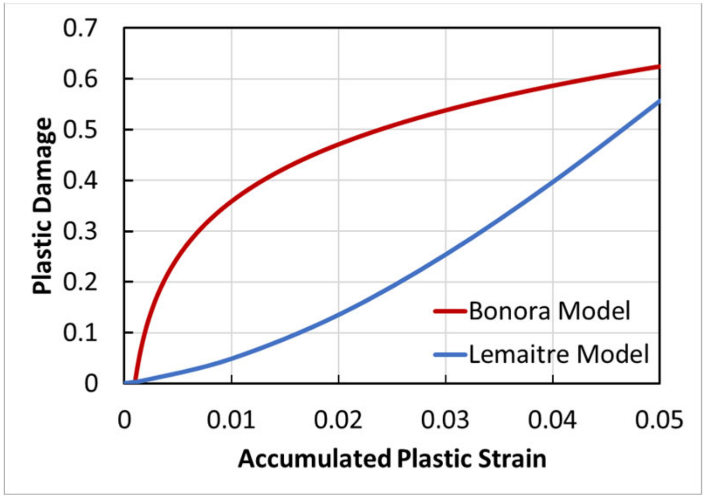

$\Delta\bar{\epsilon}_p$: depends on the initial dent damage

Bonora plastic damage formula

$$\boxed{\frac{dD^p}{dN} = D_o + (D_{cr} - D_o)\left(1 - \left(1 - \frac{\ln(\Delta\bar{\epsilon}_p/\epsilon_{th})}{\ln(\epsilon_{cr}/\epsilon_{th})}R_v\right)^{\eta}\right)}$$

$$R_v = 2(1+\nu)/3 + 3(1-2\nu)(\sigma_H/\sigma_{eq})^2$$ triaxiality function

Task-4.3 Implementation of a User-material Subroutine in Abaqus

- ✓ **The model implemented into a user-material subroutine (UMAT) in ABQUS FEA**

Model calculates stress and strain fields, then estimate damage

Damage controls stiffness degradation

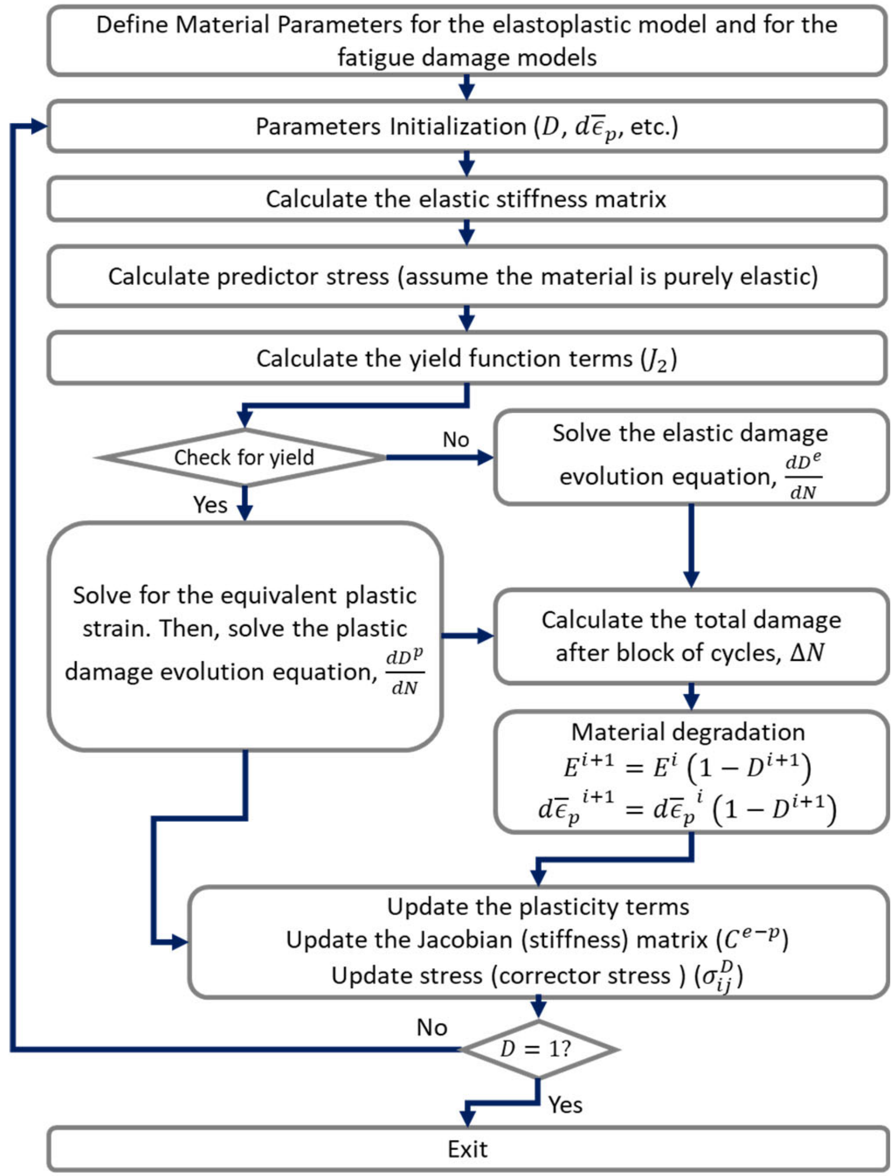

Task-4.4 Model Calibration/Verification

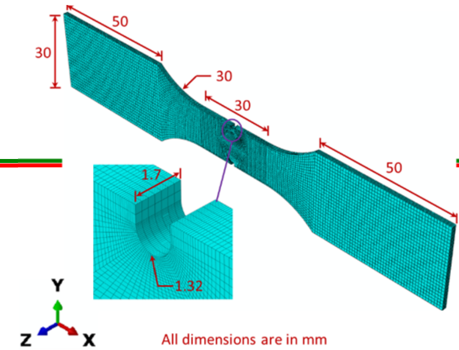

$$D = D_p + D_e$$

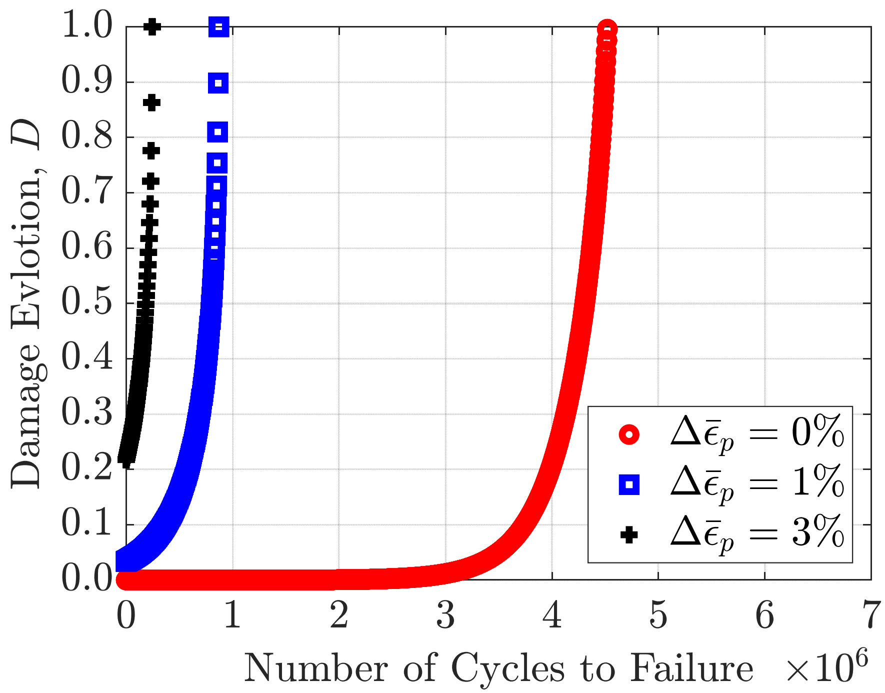

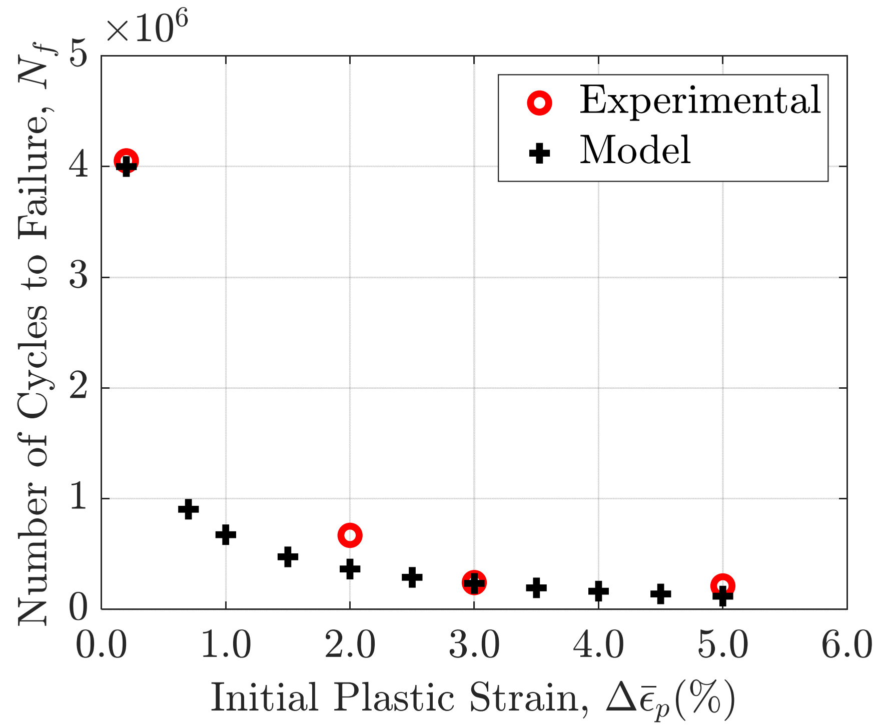

Conditions: $\sigma_{max} = 0.6\sigma_y$ **MPa and** $R = 0$

Experimental data: G. Xi, et. al, Materials & Design, 194, 2020.

Task-4.5 HC Fatigue Model Implementation

To save the computational time, two different techniques are employed

1. Simplified solution algorithm

- ✓ Compute the stress state at the maximum point in cycle.

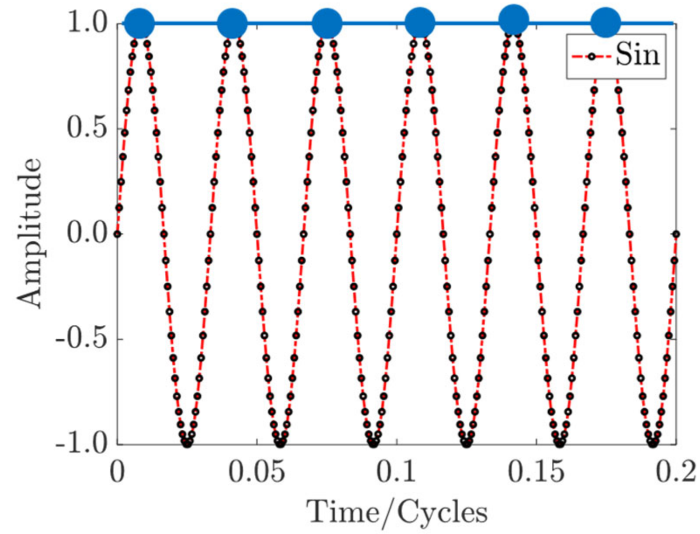

2. Cycle jumping technique

- ✓ Assume the stress and the damage will be constant over a block of cycles

$$D^{i+1} = D^{i} + \left(\frac{dD_e}{dN} + \frac{dD_p}{dN}\right)\Delta N$$

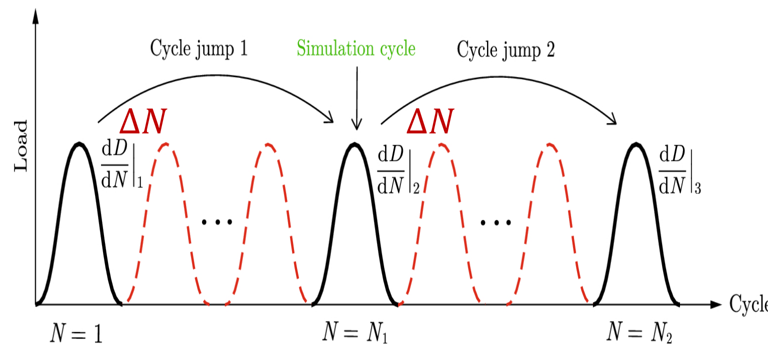

Task-4.5 Validation: (a) Simplified Solution with Cycle Jumps

damage progression

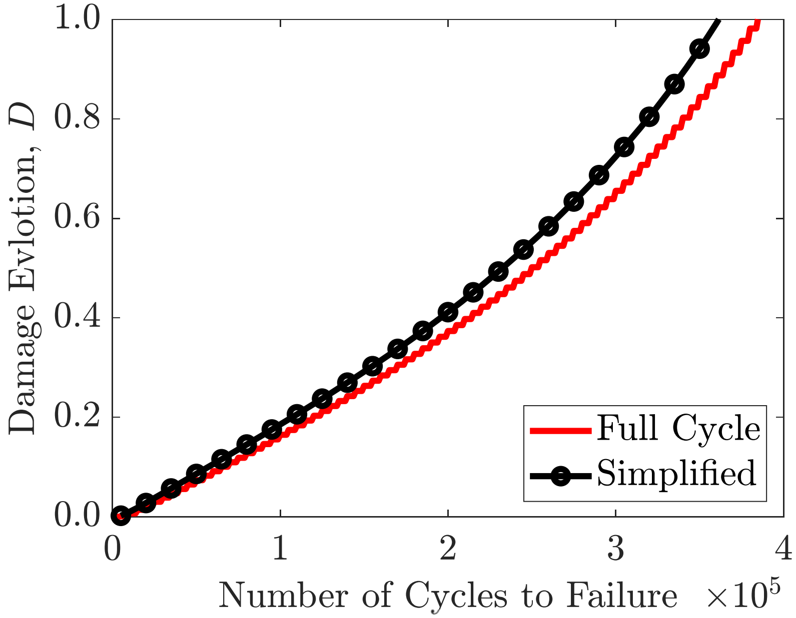

stress history

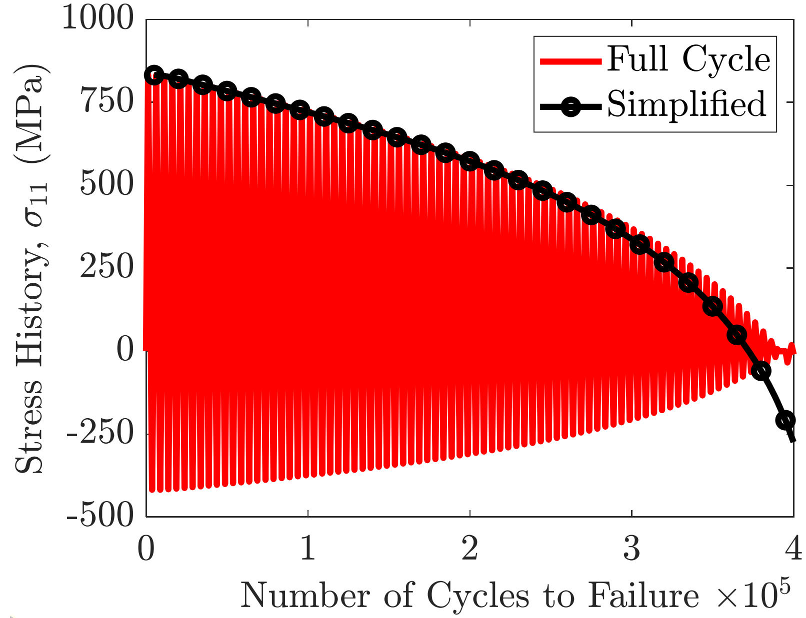

Simplified solution

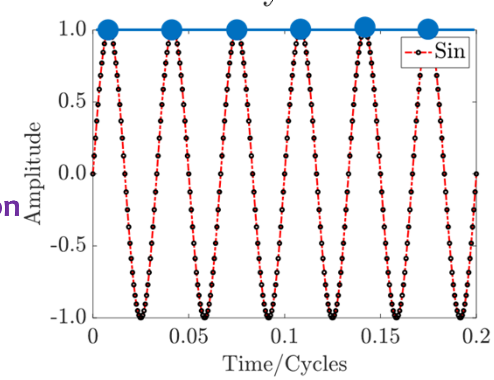

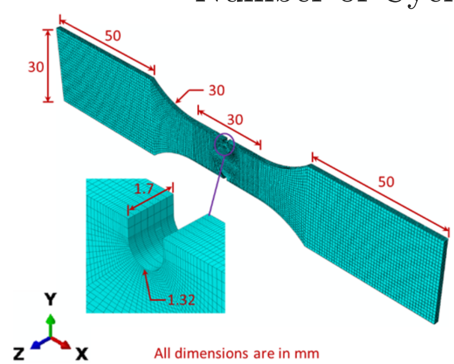

$\sigma_{max} = 800$ MPa
$R = -0.5$

Task-4.5 Validation: (b) Monotonic Dent Loading

material parameters for the pipeline steels

	Parameter	E (GPa)	σ_y (MPa)	σ_u (MPa)
Legacy	**X52**	200	400	567
Modern	**X70**	200	500	620

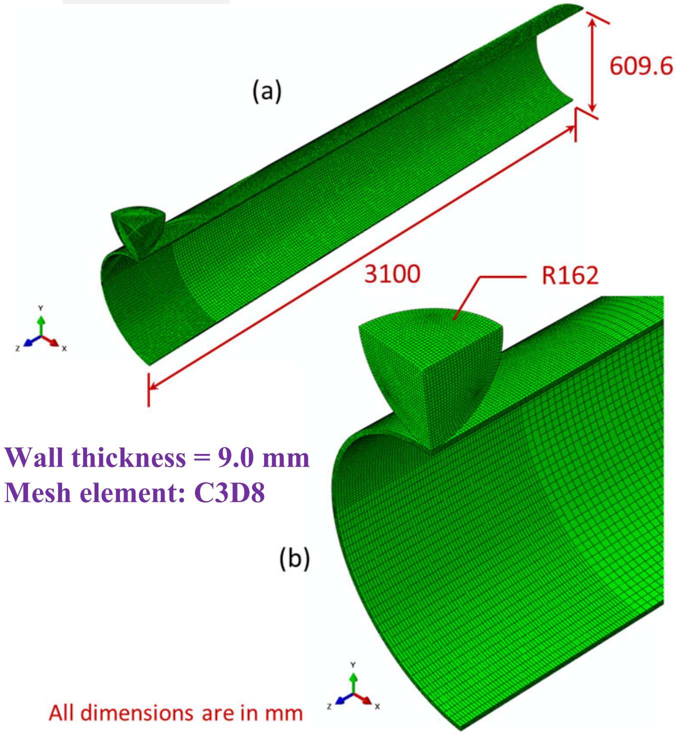

Pipe indentation model

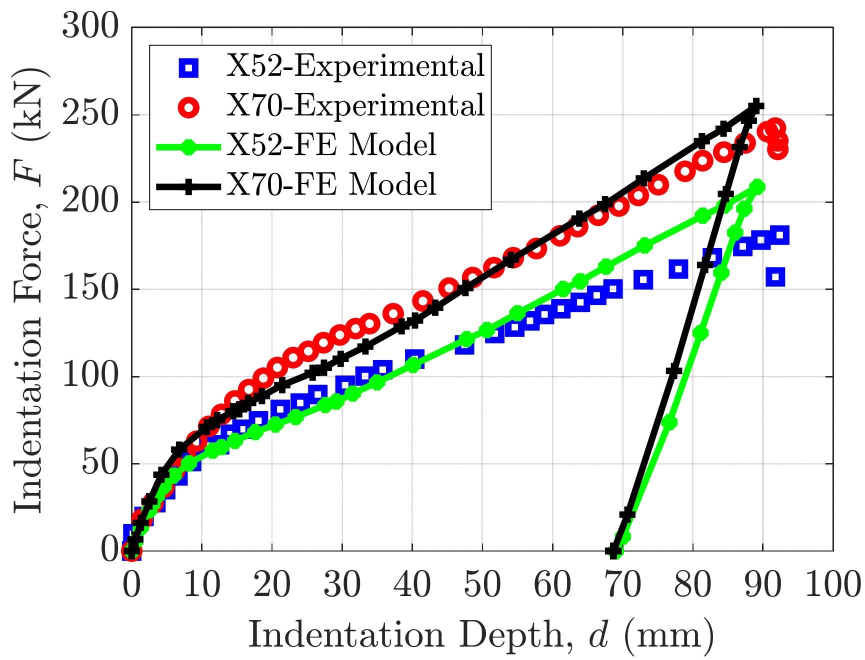

Monotonic load-indentation depth

Experimental data: Bolton et al., IPC 44205, 2010

Task-4.5 Validation: (c) Elastic Fatigue Damage model (uniform ε_e)

fatigue parameters for the tested materials

Parameter	a	b_1	b_2	β	M_o(MPa)	σ_{lo}(MPa)
X52	0.75	1.32	1.76	3.22	9341	284
X70	0.72	1.28	1.15	3.25	18357	300

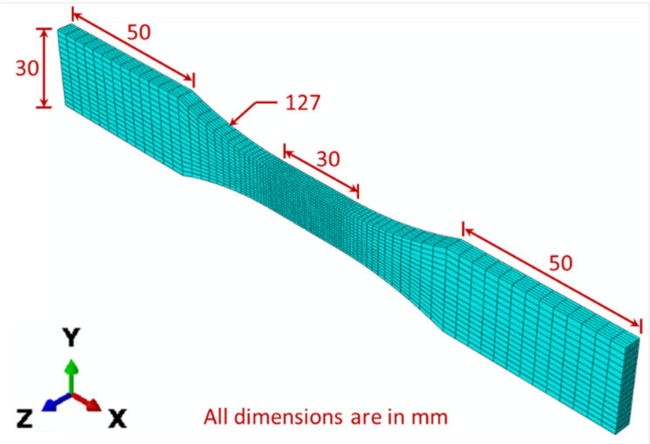

Tensile fatigue specimen

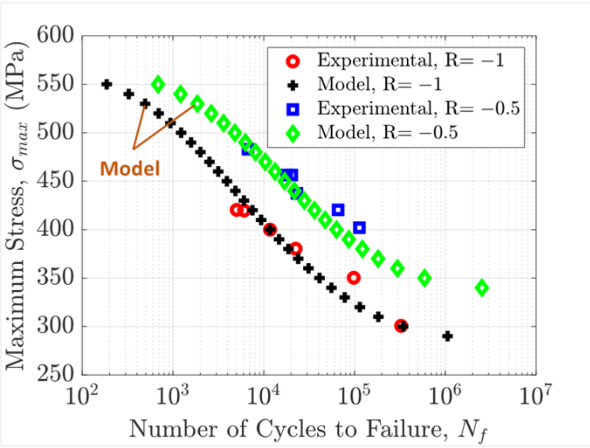

SN curve for X52

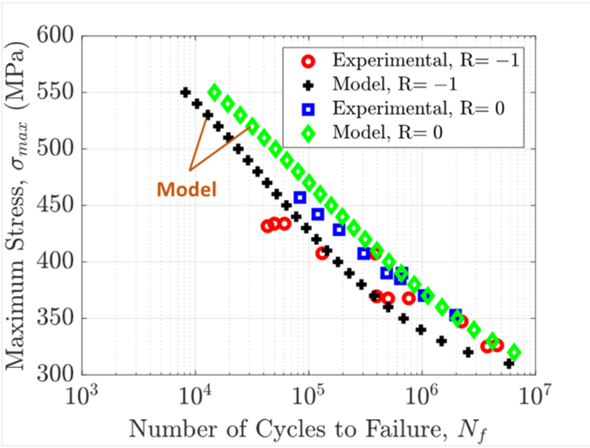

SN curve for X70

Experimental data: Md Liakat Ali, PhD Thesis, LSU, 2015.
Turhan, et al., Journal of Failure Analysis and Prevention, 20, 2020.

Task-4.5 Validation: (d) Plastic Fatigue Damage model (uniform ε_p)

Bonora plastic damage formula

$$\frac{dD^p}{dN} = D_o + (D_{cr} - D_o)\left(1 - \left(1 - \frac{\ln\left(\Delta\bar{\epsilon}_p/\epsilon_{th}\right)}{\ln(\epsilon_{cr}/\epsilon_{th})} R_v\right)^{\eta}\right)$$

Parameter	D_o	D_{cr}	ϵ_{th}	ϵ_{cr}	η
X70	0	0.48	0.004	0.30	0.680

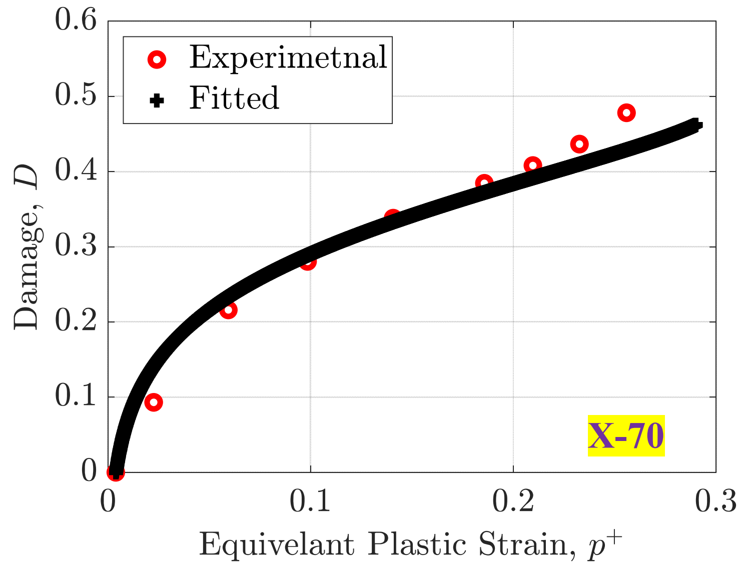

Experimental data: Lee at al., Acta materialia, 54(4), 2006

Task-4.6 Simulation Sequence: (a) Indentation

Figure 1 Picture of pipeline dent (Source: https://www.google.com/imghp?hl=en)

- Indentation (step-1)

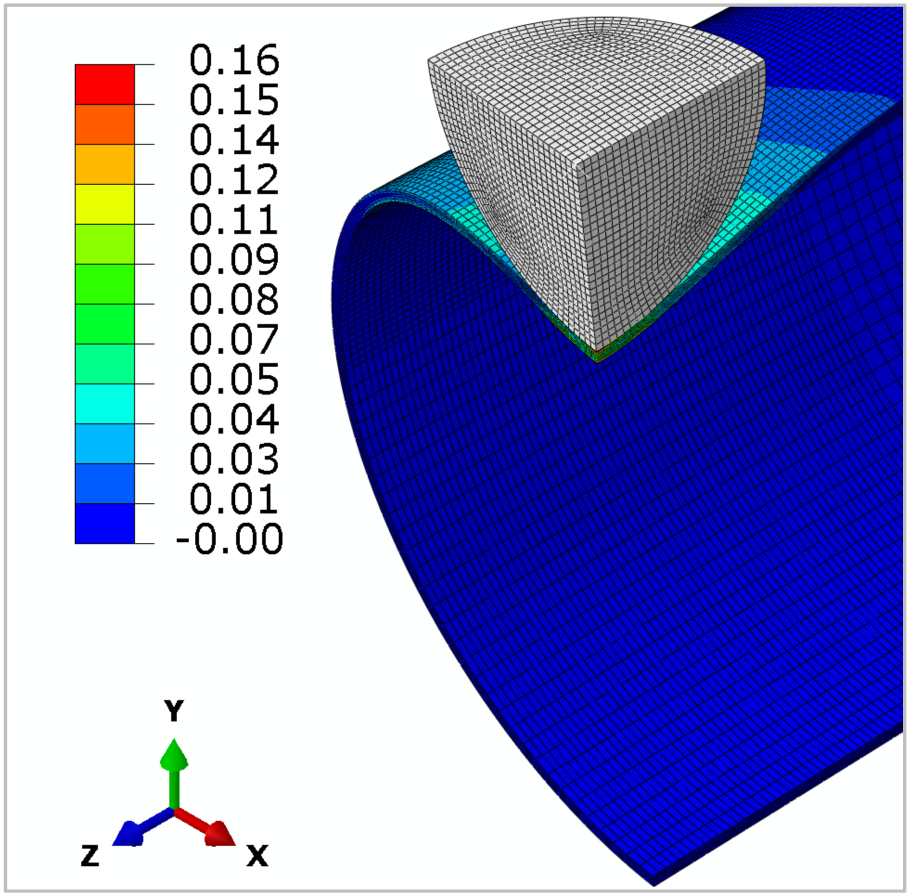

Contours of equivalent plastic strain

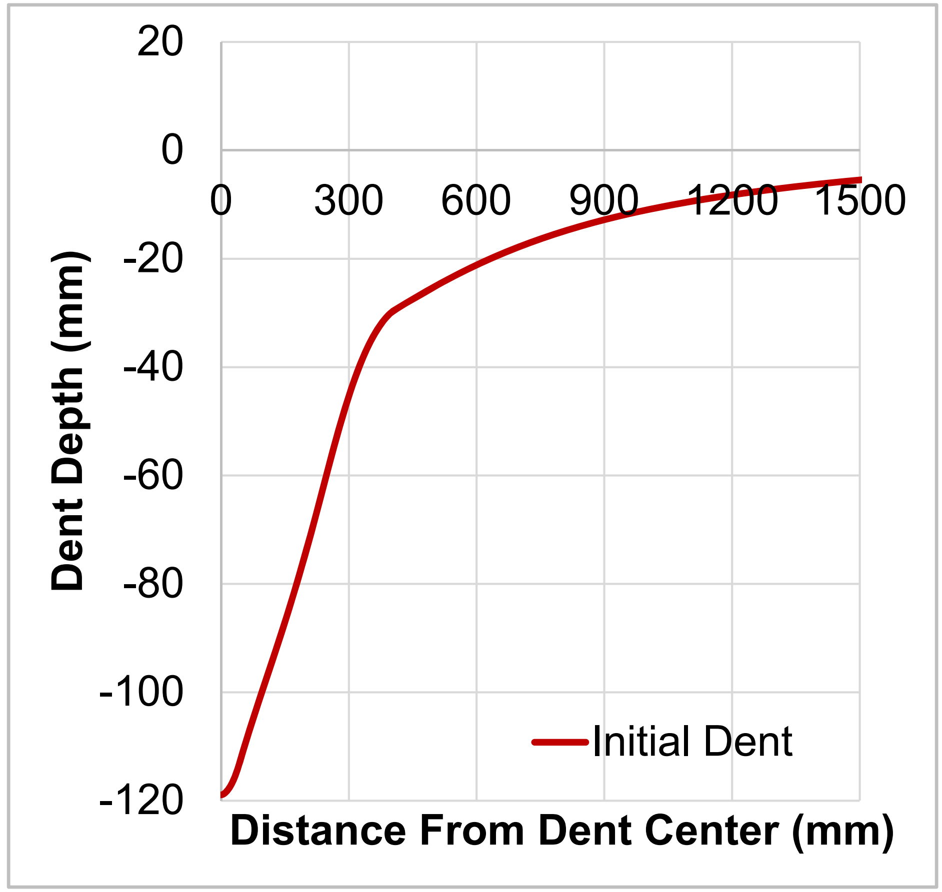

Axial dent profile

Task-4.6 Simulation Sequence: (b) Indentation Elastic Unloading

❖ **Elastic recovery or indentor removal (step-2)**

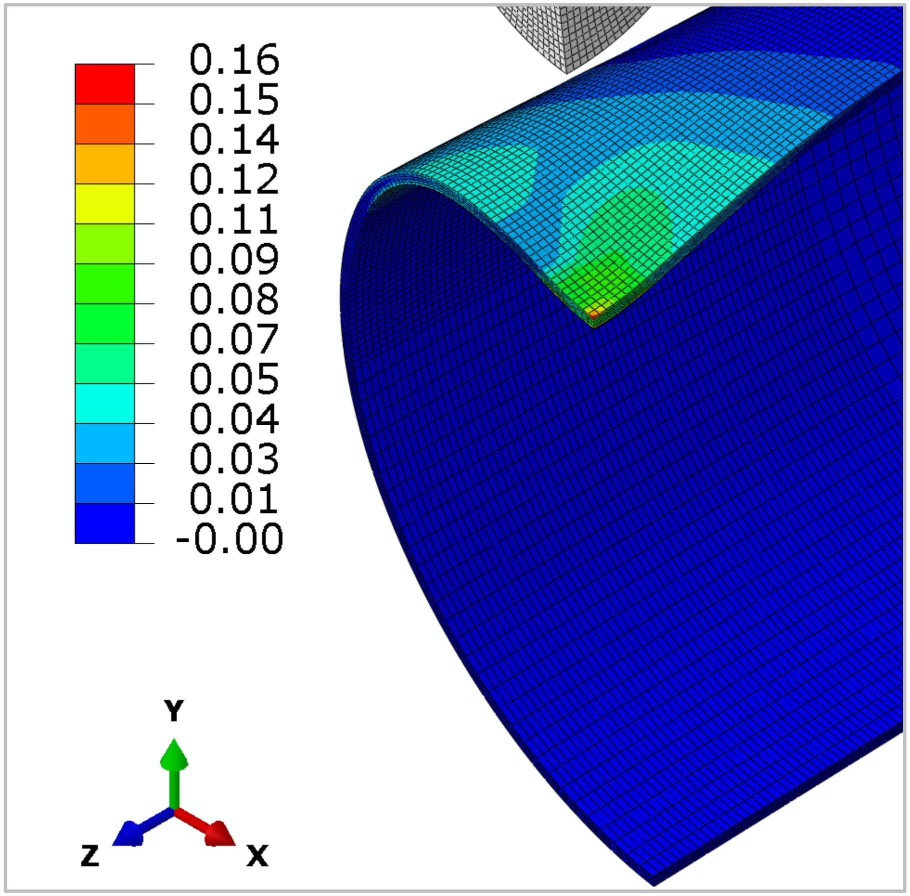

Contours of equivalent plastic strain

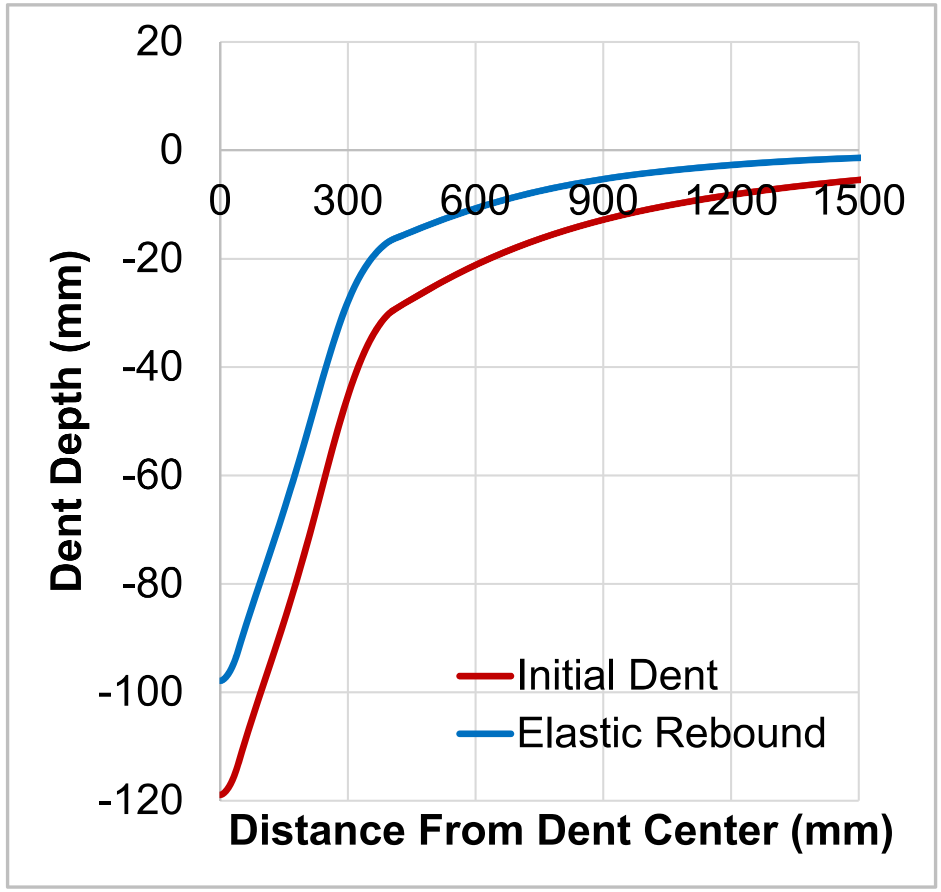

Axial dent profile

Task-4.6 Simulation Sequence: (c) Pressure Rebounds

❖ **Pressure rebounding (step-3)**

$$\frac{dD^p}{dN} = D_o + (D_{cr} - D_o)\left(1 - \left(1 - \frac{\ln(\Delta\bar{\epsilon}_p/\epsilon_{th})}{\ln(\epsilon_{cr}/\epsilon_{th})}R_v\right)^\eta\right)$$

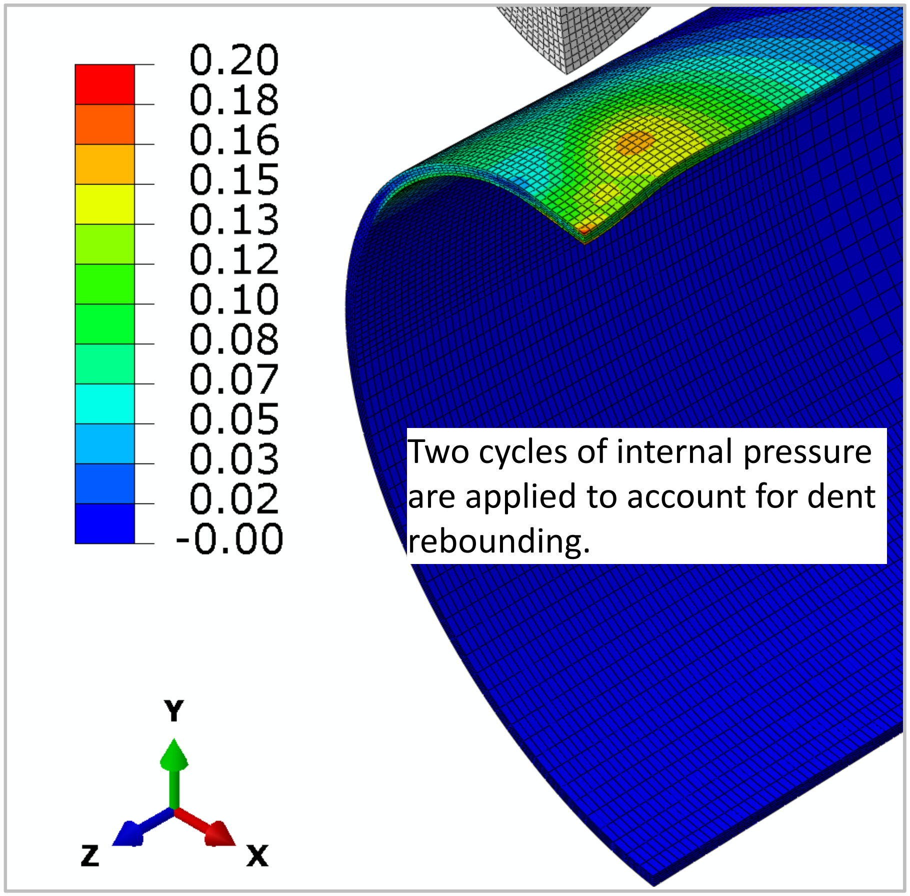

Contours of equivalent plastic strain

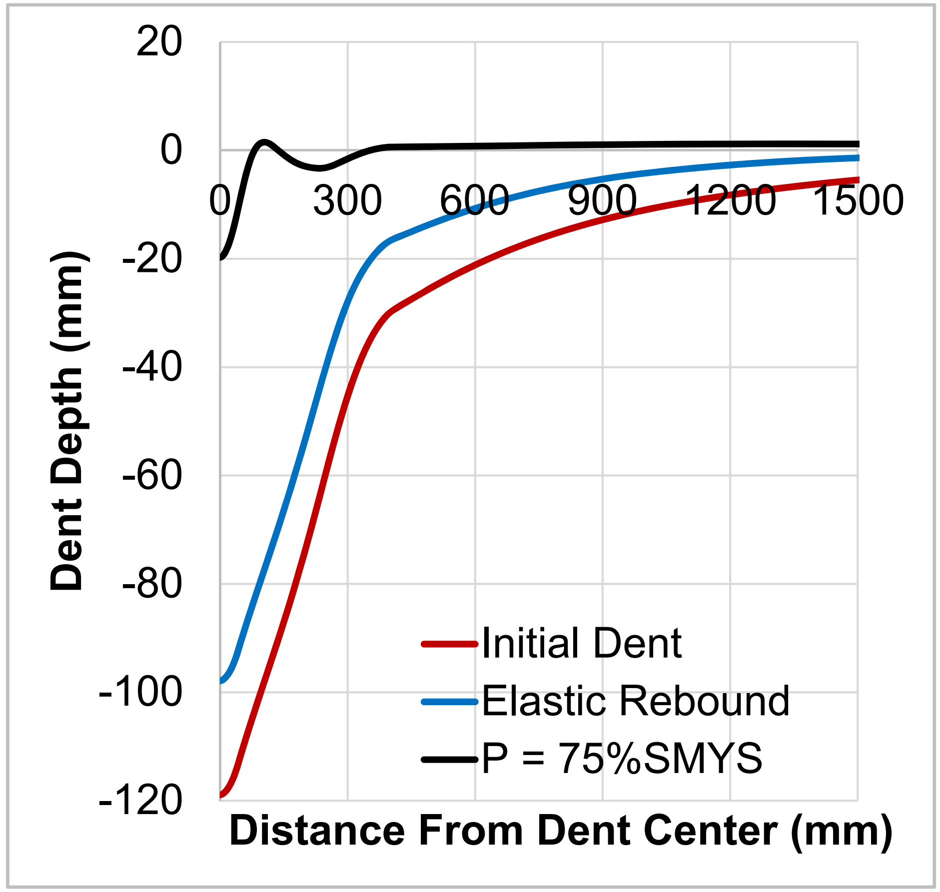

Axial dent profile

Task-4.6 Simulation Sequence: (d) Cyclic Pressure Loading

- **Cyclic pressure or fatigue loading (step-4)**

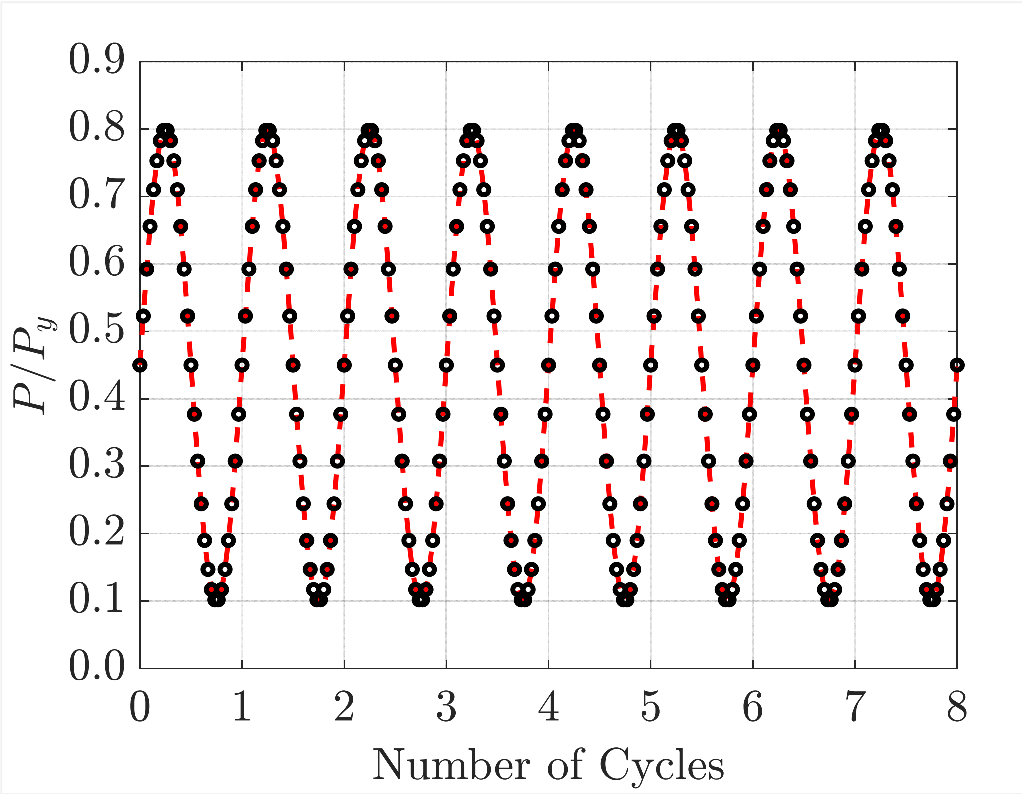

The applied cyclic fatigue loading (R = 0.125)
P = 10% – 80% SMYS

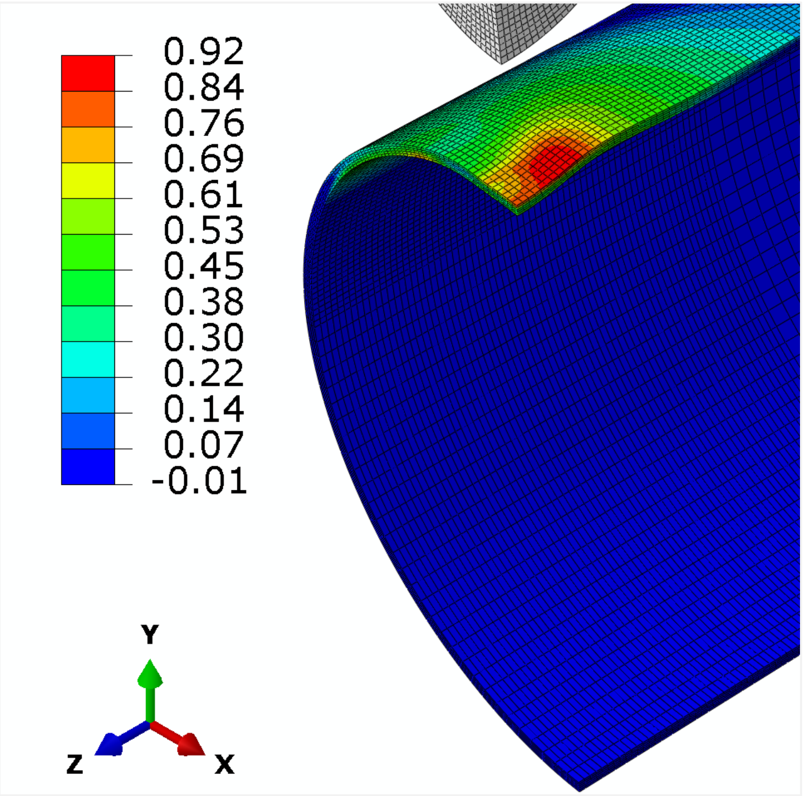

The computed fatigue damage
after load application

Task-4.6 Simulation Sequence: (f) Identify Failure/Cracking Patterns

❖ **Crack pattern by element deletion**

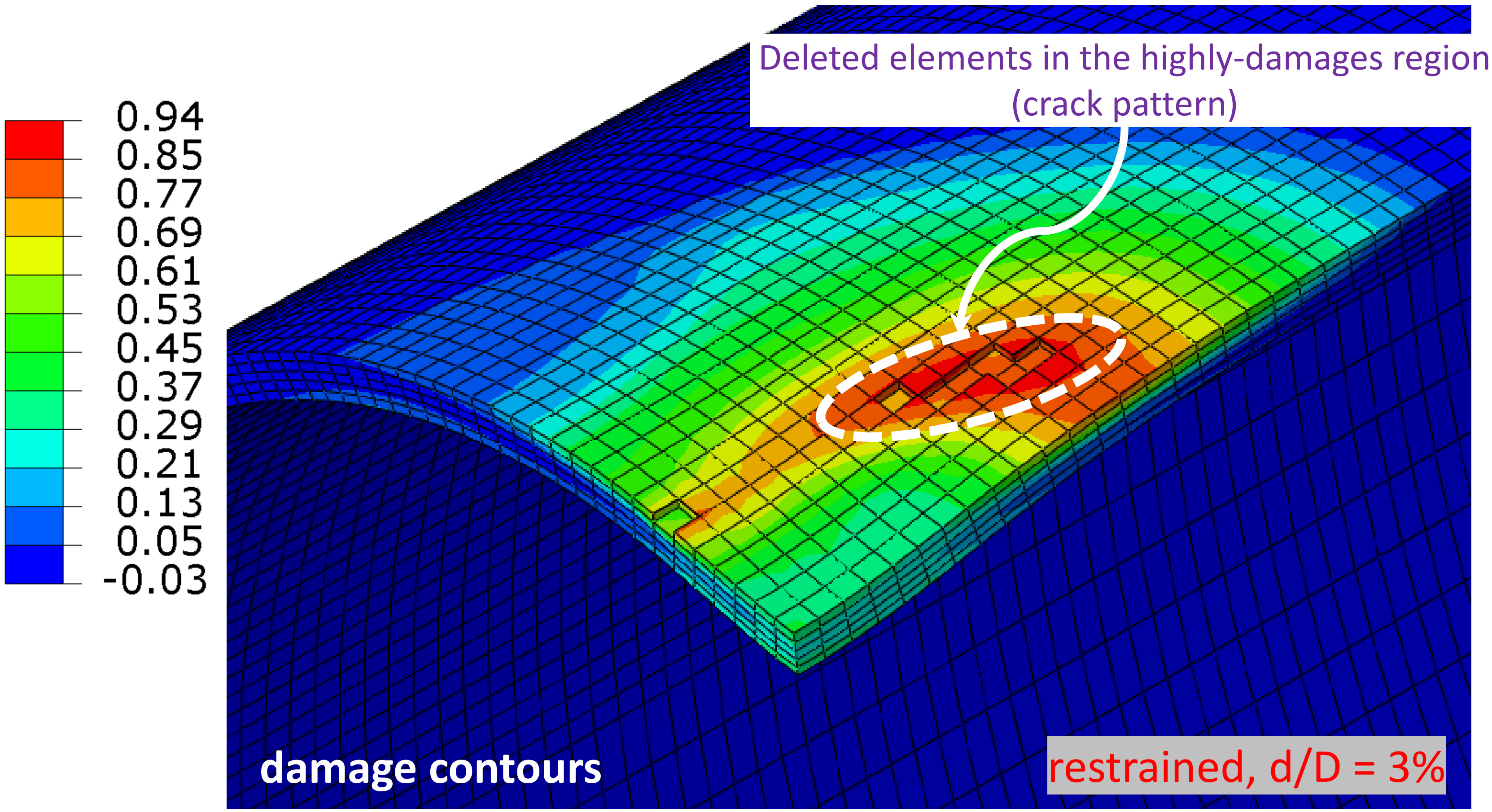

Task-4.6 Simulation Sequence: (e) restrained Pipe

- ✓ For a restrained pipe, the indentor was kept in place after the elastic recovery step
- ✓ dent rebounding
- ✓ fatigue loading is applied
- ✓ damage is computed

The applied cyclic fatigue loading (R = 0.125)
P = 10% – 80% SMYS

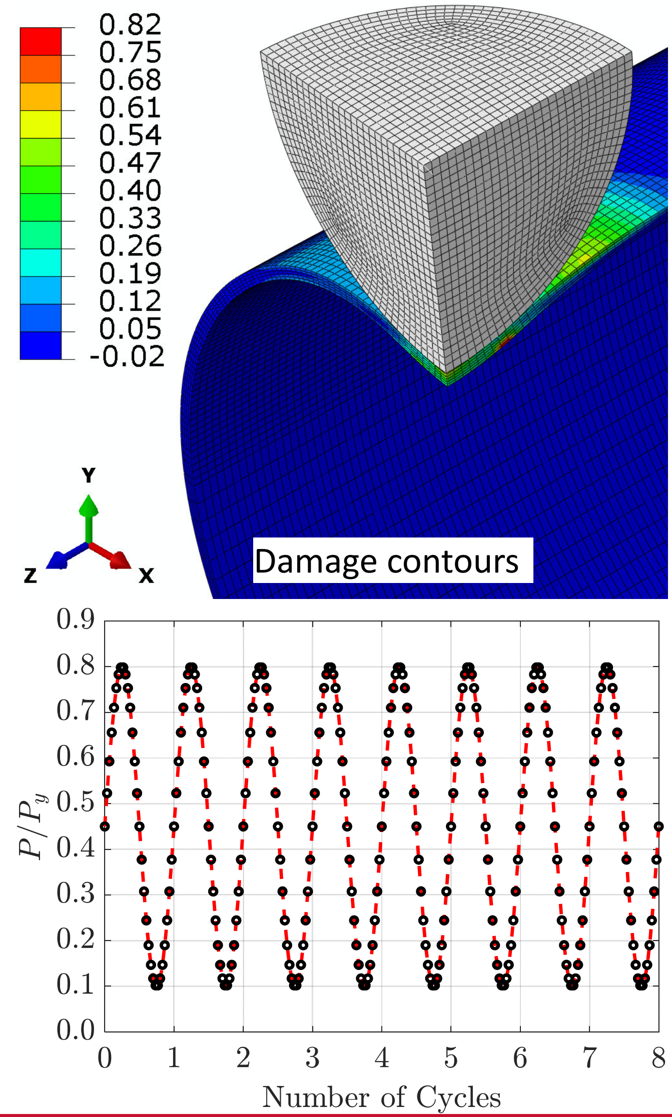

Results: (a) Shallow **Unrestrained** Dent— outer, axial

❖ Unrestrained dents

- ✓ Fatigue cracks are initiated axially on the outer surface of the pipe
- ✓ The crack appears on the shoulder of the dent and propagates closer to center of the dent

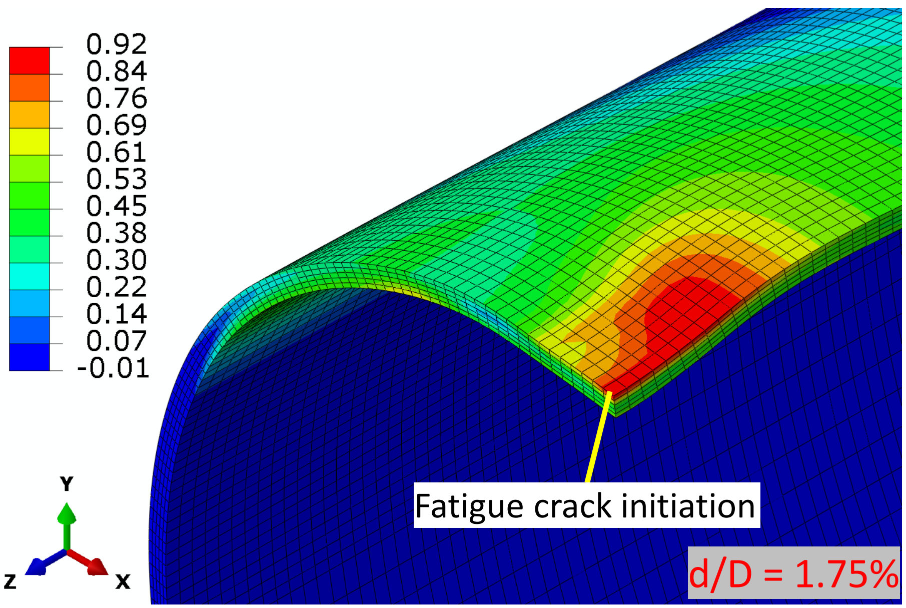

Contours of the damage index

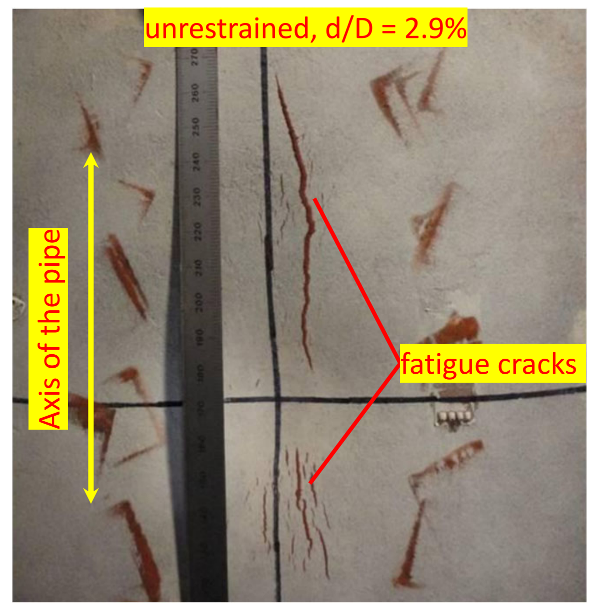

X52, OD = 457 mm and t = 7.9 mm

Experimental data: Tiku, et al., IPC 45134, 2012

Results: (b) Shallow **Unrestrained** Dent-Comparison with Full-Scale

- **Fatigue response of full-scale pipe**

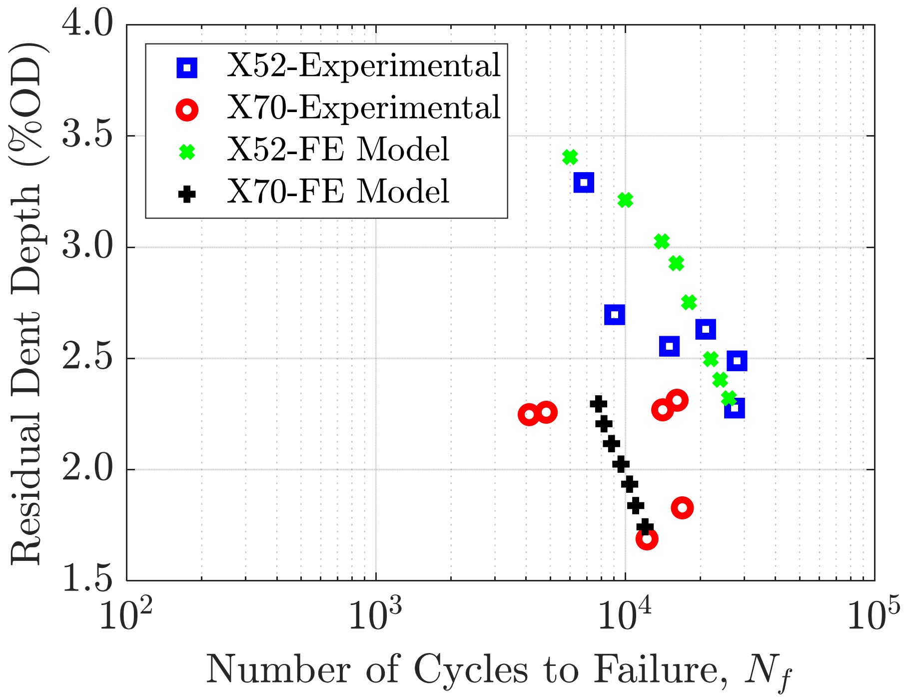

Fatigue life at different dent depths

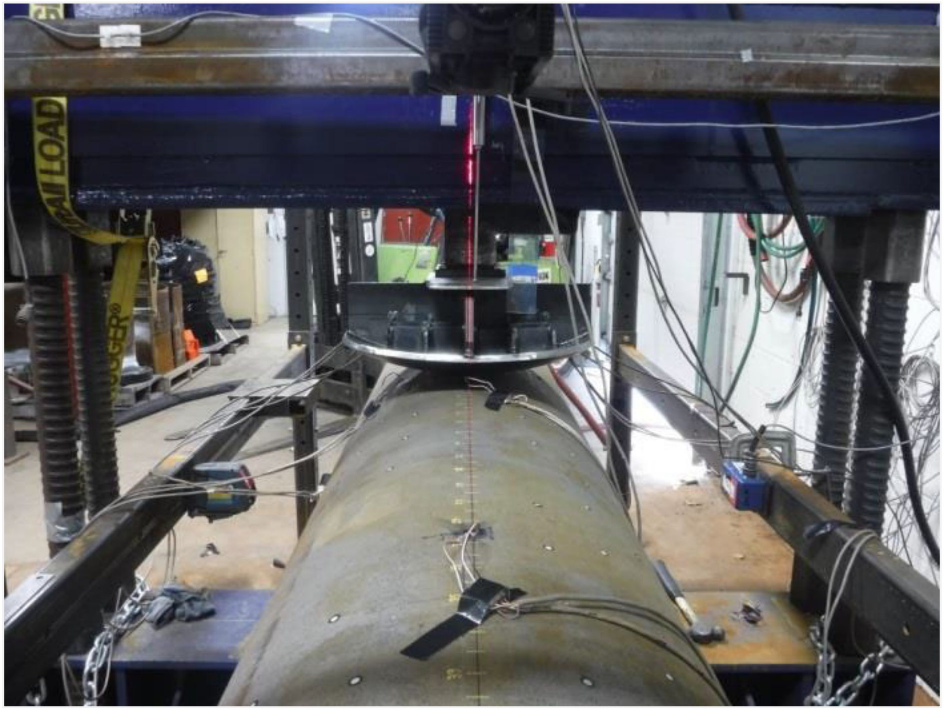

Full-scale experimental testing setup

Experimental data: Bolton, et al., IPC 44205, 2010

Results: (c) Shallow **restrained** Dent — outer, radial

❖ Shallow restrained dents

- ✓ Fatigue cracks appear on the shoulder of the dent, which are circumferentially initiated on the outer surface of the pipe
- ✓ The azimuthal orientation of the crack is modulated by the depth of the dent such that the crack becomes closer to the axial center of the pipe as the depth increases.

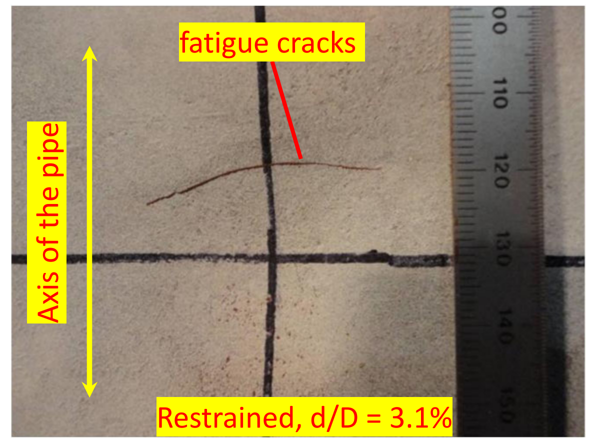

X52, OD = 457 mm and t = 7.9 mm

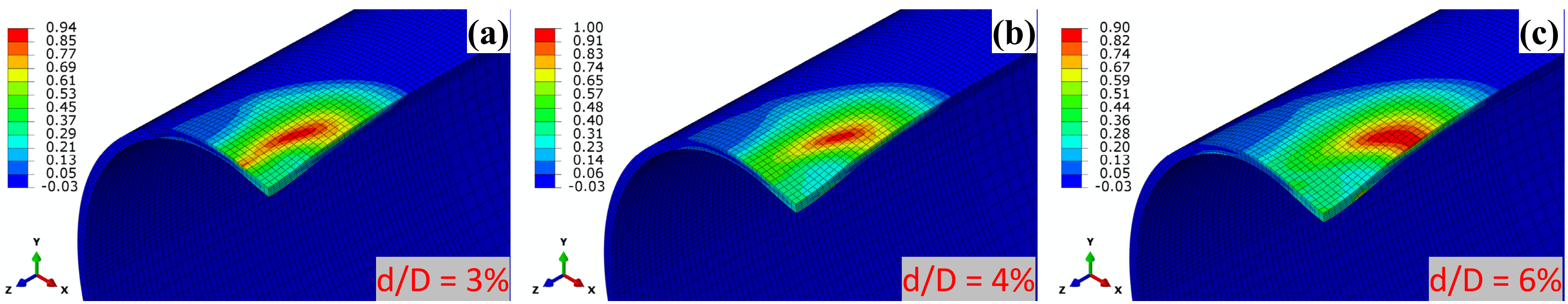

Contours of the damage index

Experimental data: Tiku, et al., IPC 45134, 2012

Results: (d) Deep **restrained** Dent — inner, radial

- **Deep restrained dents**
  - ✓ Fatigue are circumferentially initiated on the inner surface of the pipe
  - ✓ The initiation point is observed to be at the contact point between the indentor and the pipe

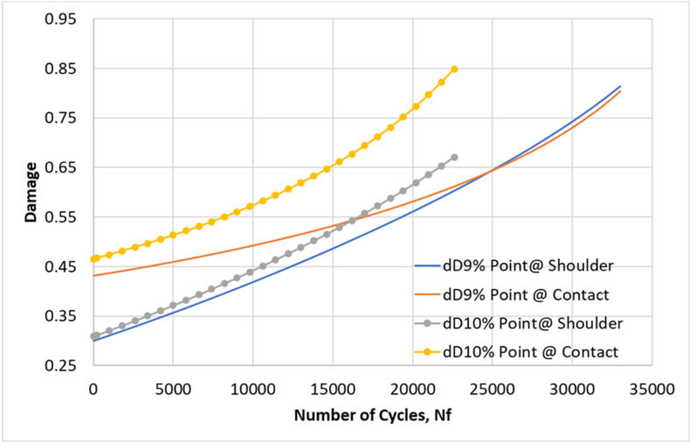

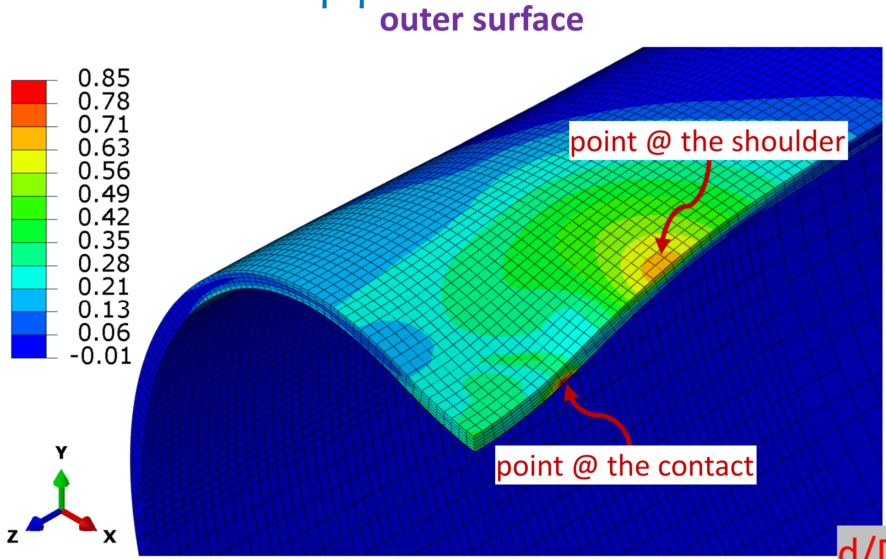

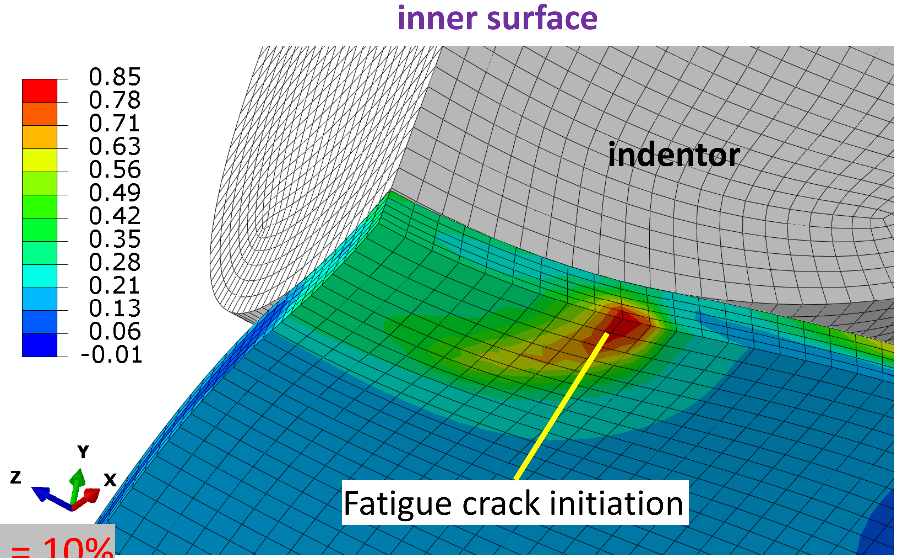

d/D = 10%

Contours of the damage index

Results: (e) Fatigue Life X-70 Steel **restrained vs Unrestrained** Dent

❖ Model Derived Fatigue Response

- ✓ Fatigue life of a defect-free pipe is ~ **5** M-cycle.
- ✓ For $h/D = 3\%$, fatigue life is reduced to just **1.5%** of the undamaged life.
- ✓ Unrestrained residual depth after pressure rebound from dent of $h/D = 15\%$.

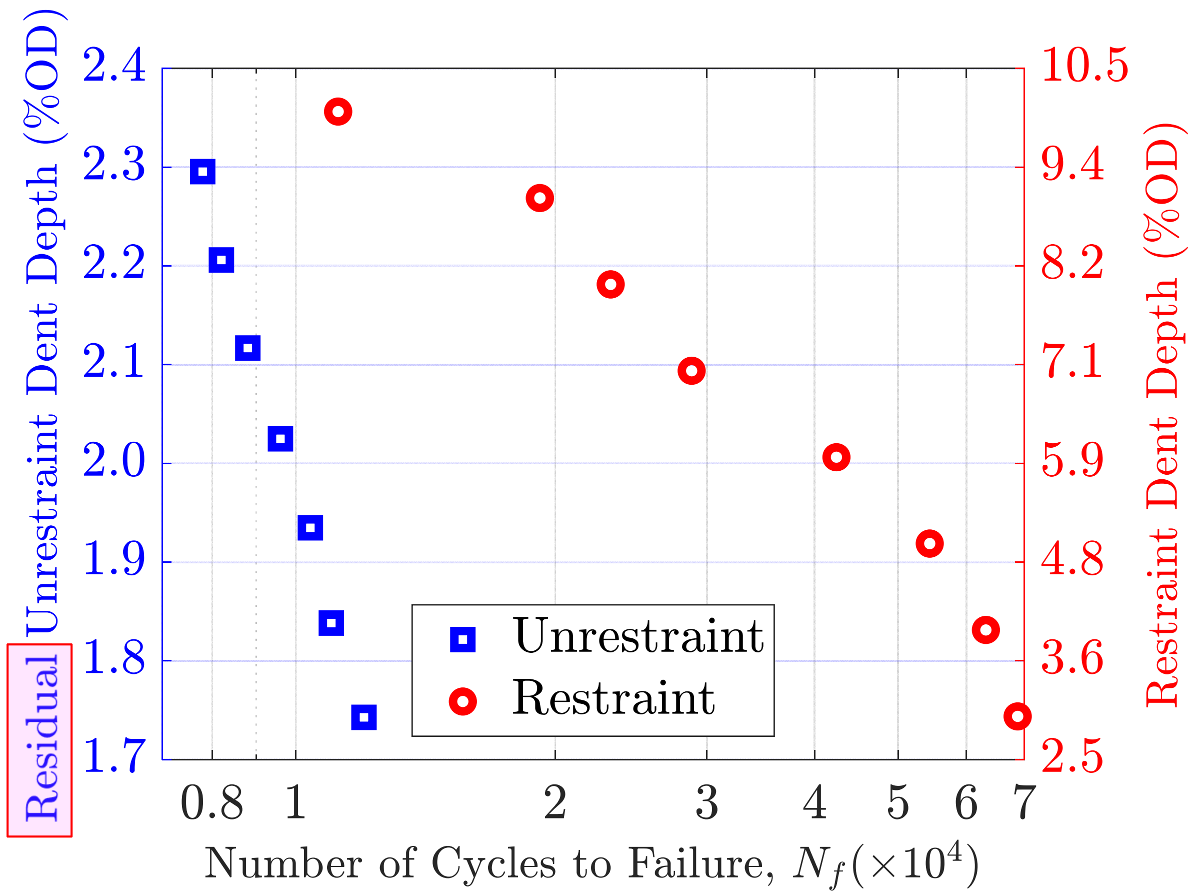

- ➢ restrained dents show higher fatigue lives compared to unrestrained dents

Results: (f) Synergistic Plastic Damage restrained/Unrestrained Dent

❖ Initial plastic damage

- ✓ Excessive initial damage due to pressure-driven rebounding leading to shorter fatigue life in the unrestrained cases.

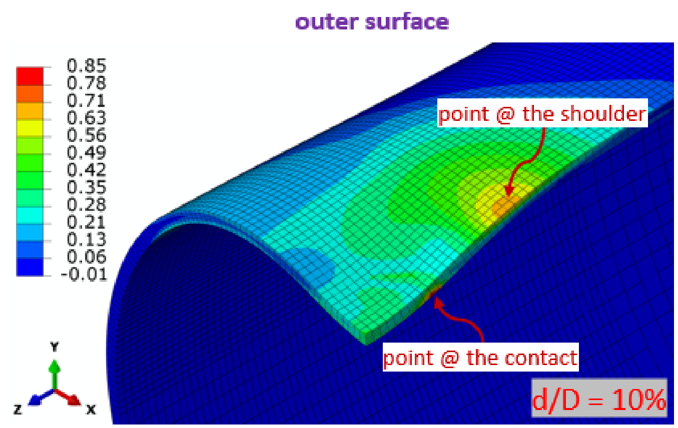

Restrained @ fixed spatial point in the axial path

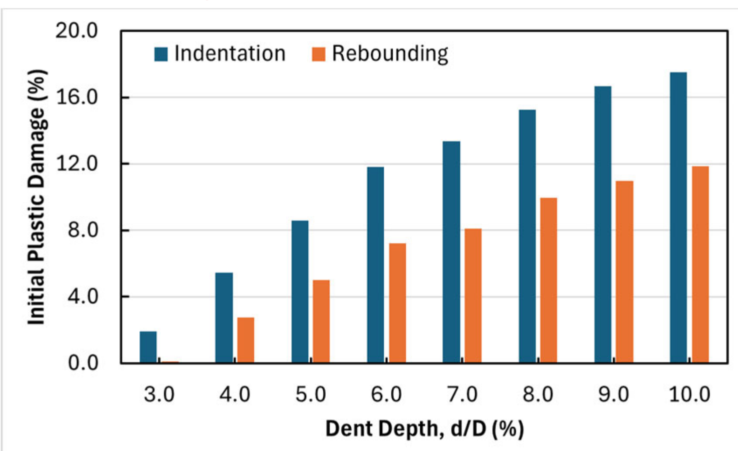

Unrestrained (15% OD initial indentation

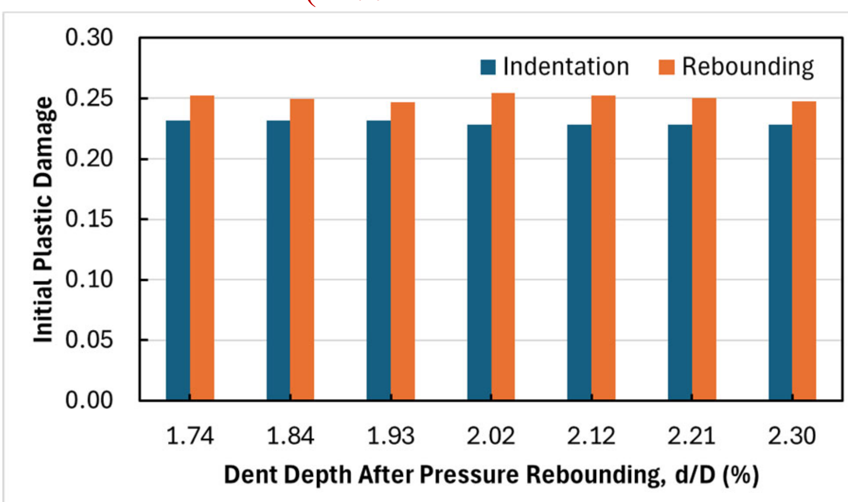

Results: (g) Synergistic Dent/Rebound Accumulated Plastic Strains

- Location of the failure point (strain profile along the axial path)

Restrained (d/D = 3%)

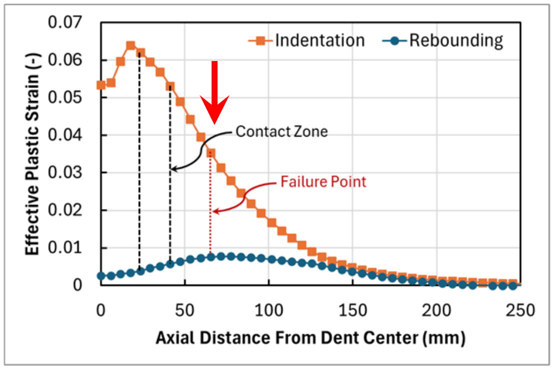

Restrained (d/D = 7%)

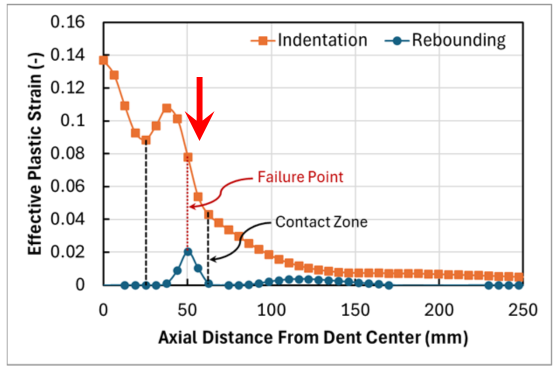

Restrained (d/D = 15%)

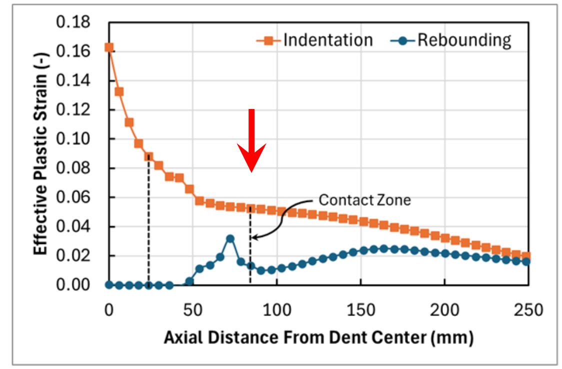

Unrestrained (d/D = 1.74%) (15% OD initial indentation depth)

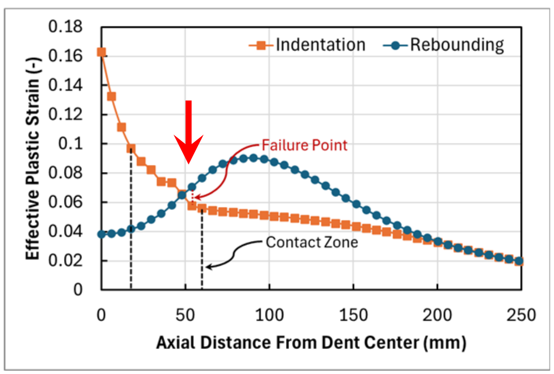

Unrestrained (d/D = 1.93%) (15% OD initial indentation depth)

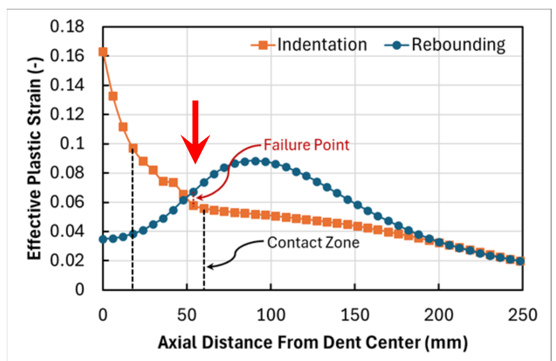

Unrestrained (d/D = 2.3%) (15% OD initial indentation depth)

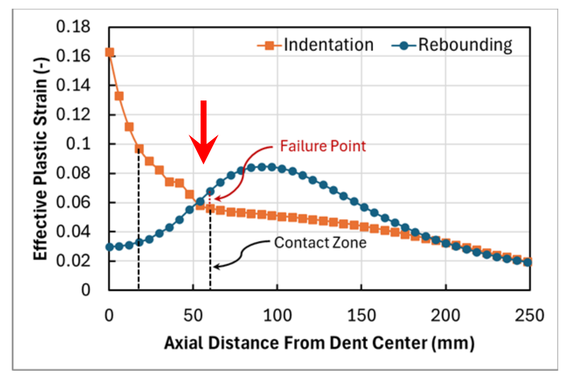

Summary of Findings: Synergistic Interactions

- ✓ Accumulated ε_p
- ? Residual Stress
- ? Geometric Effects

Pristine Pipeline (ε_p=0%) ~ 5 M-cycle

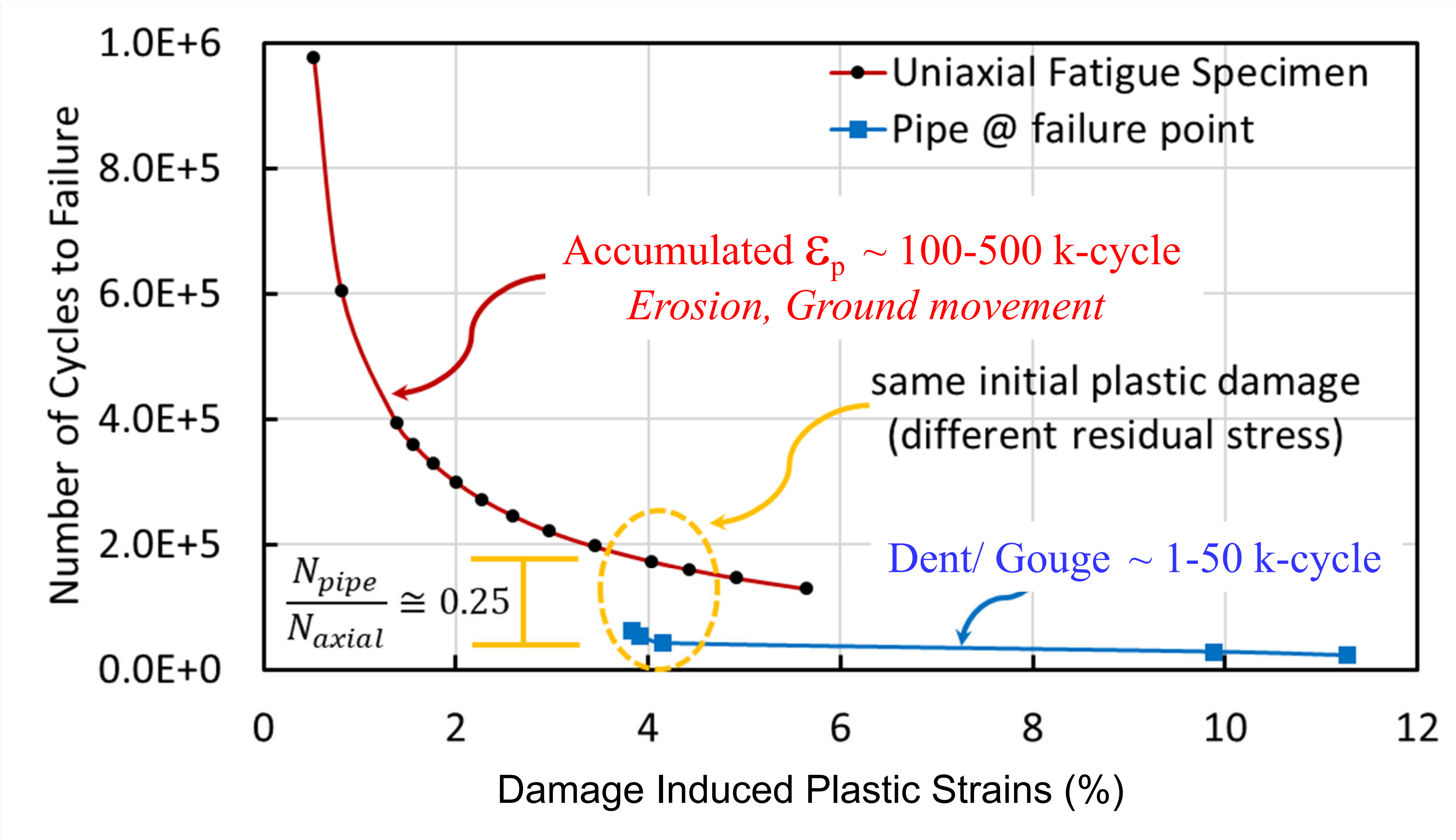

Results: (h) Synergistic Dent/Rebound Accumulated Residual Stresses

❖ **Residual stress after pressure rebounding,**

shifted the mean stress amplitude

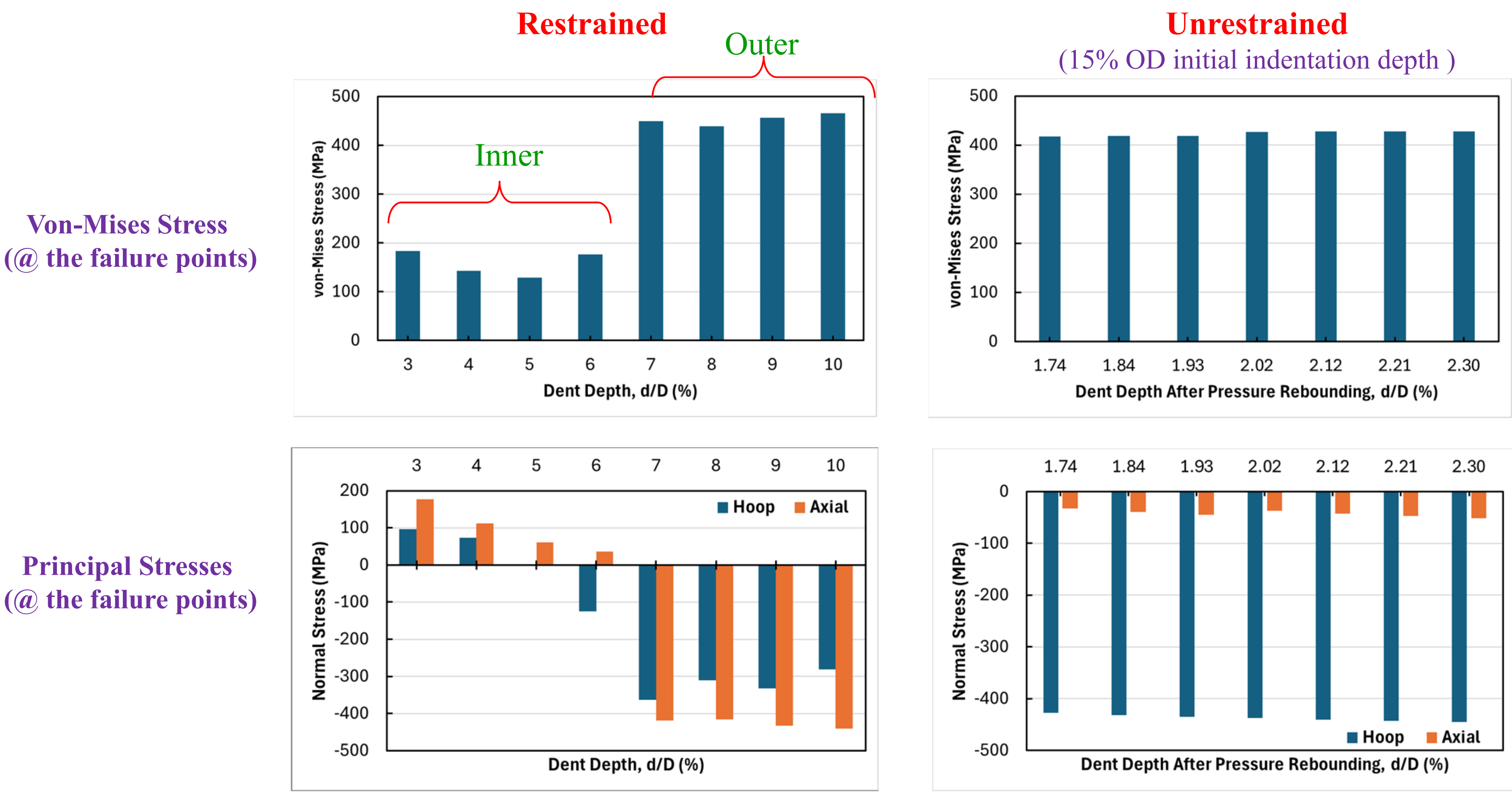

Results: (g) Synergistic Geometry induced Stress Amplitude Riser, SCF

❖ **Stress Concentration Factor**

✓ SCF is obtained by dividing the stress amplitude at the failure point over the remote stress amplitude (at a point far from the dent).

✓ Higher SCF (~20% on average) in the unrestrained conditions because of pressure-driven rebounding.

✓ The stress magnification in the dented area reduce the fatigue life by ~ 28% at the same level of initial plastic damage.

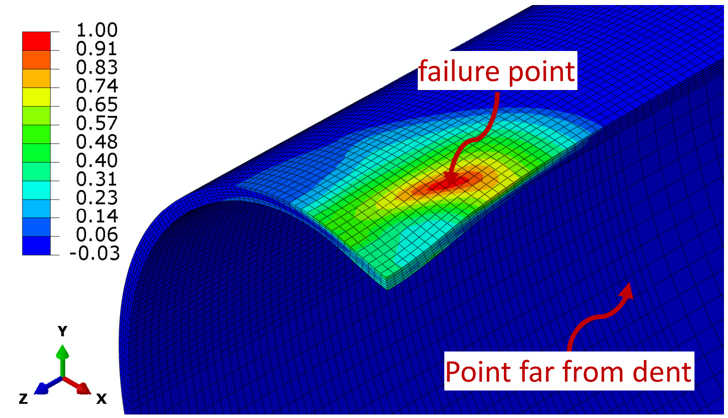

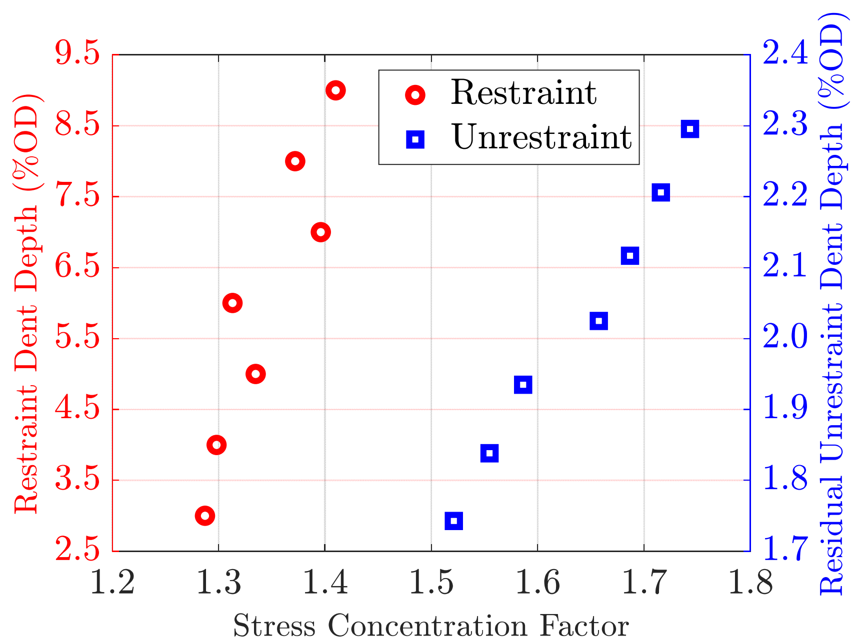

Summary of Findings: Synergistic Interactions

- ✓ Accumulated ε_p
- ✓ Residual Stress
- ✓ Geometric Effects

Pristine Pipeline (ε_p=0%) ~ 5 M-cycle

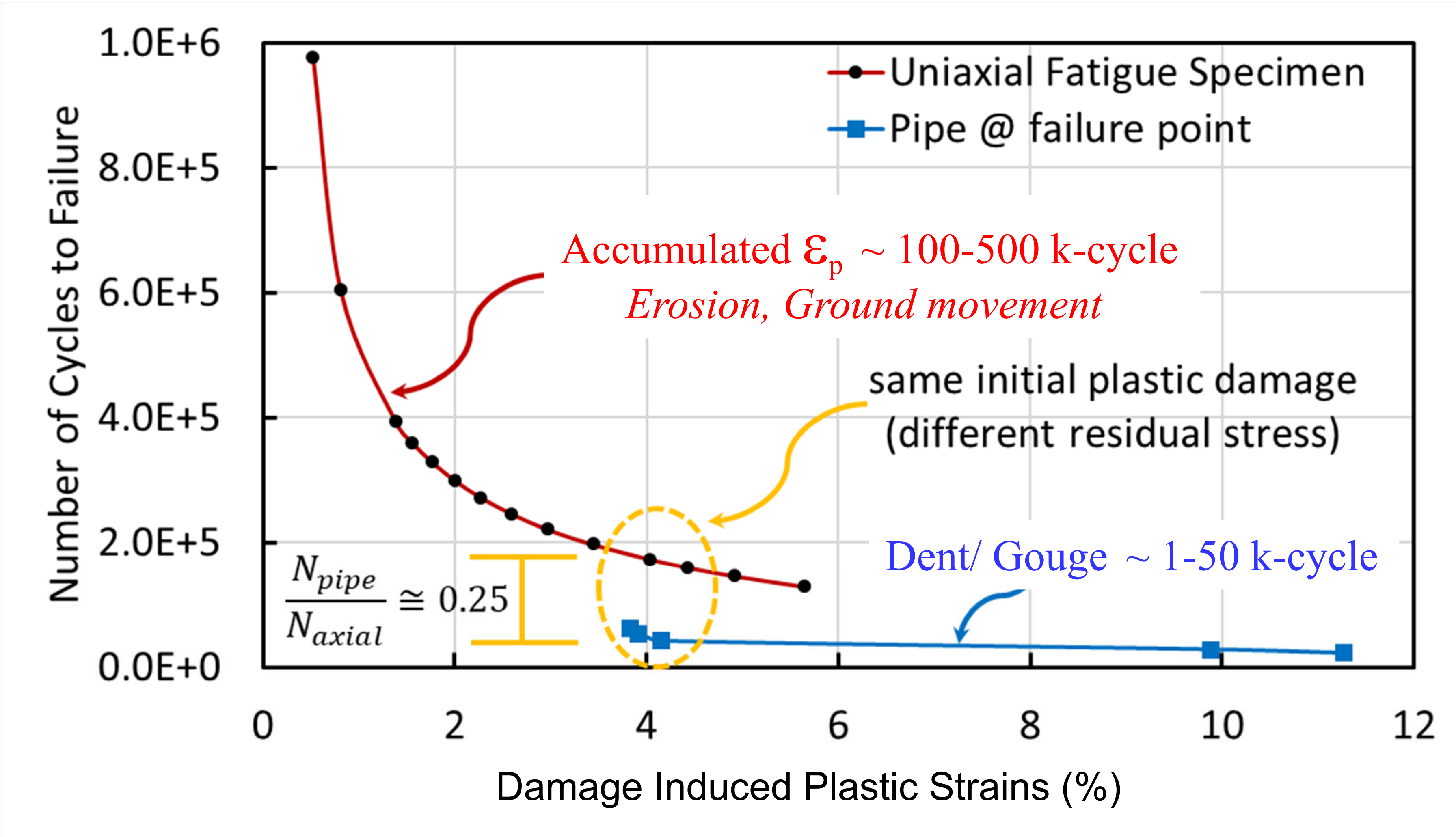

Needs to Revisit ASME B31.8

❖ **Fatigue response of restrained dents (FE)**

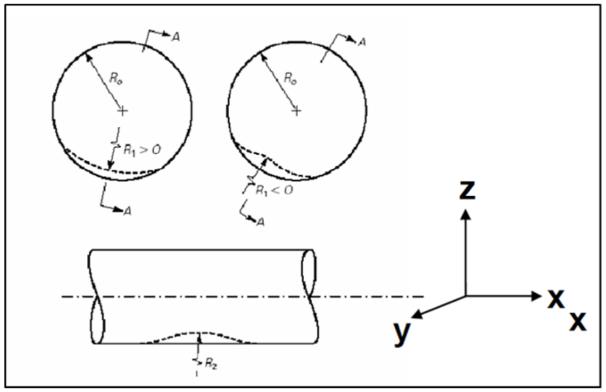

- ✓ ASME B31.8 is a profile based approached. It does not account for deformation histories or stress concentration.
- ✓ At higher dent depth, ASME B31.8 predictions are ~30% (on average) less than the localized FE results.
- ✓ This difference in strain yields in ~35% in life.

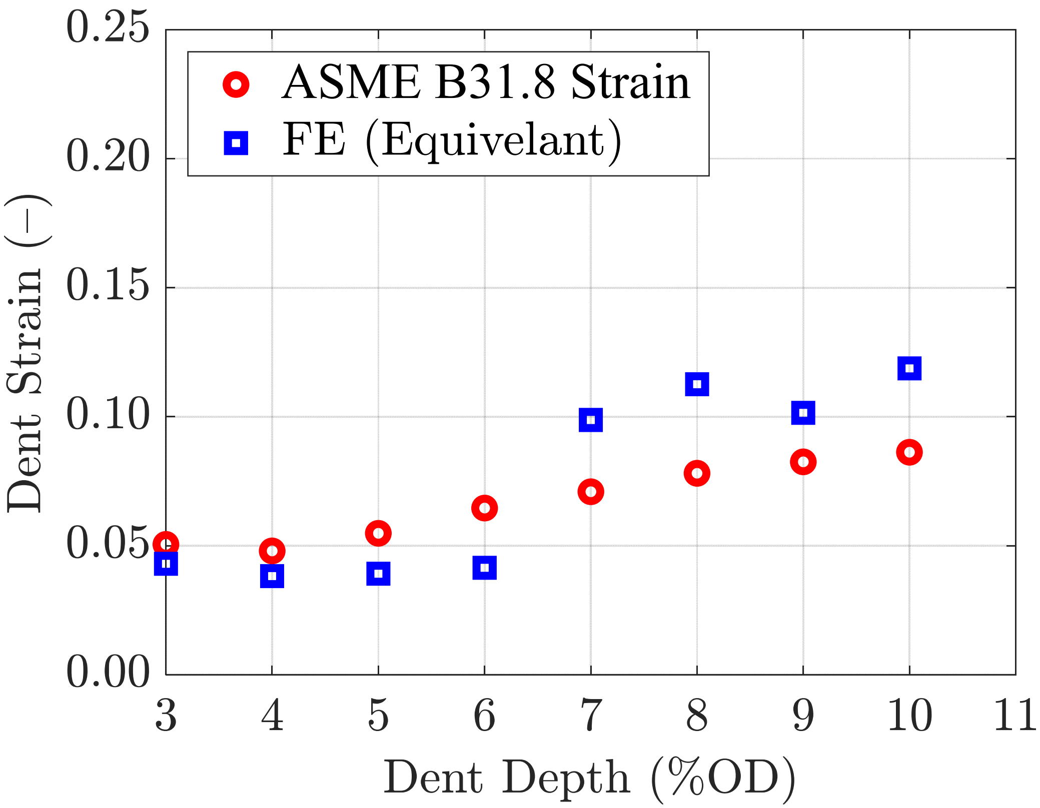

Concluding Remarks

- Developed an integrated computational tool to predict fatigue life of dented and gouged pipelines of different geometry and orientations.
- Identified different factors controlling Fatigue life of dented pipes (Residual plastic strain, residual stresses, Stress risers)
- The position and orientation of the fatigue crack are dictated by both dent conditions (restrained or unrestrained) and the depth of the dent
- Naïve assessment of chemical and mechanical coupling influence on IGC
- Level of prestrain increased the density of nucleation sites and accelerated the corrosion process.
- Progress to link GB cohesion strength with corrosion and prestrain levels.

Next Step/ Opportunities

- Extended Lab-scale investigation of coupling between residual stress, plastic strains and SCC
- Numerical Assessments of fatigue life for wide range of interactive threats
  - Different critical gouge geometries and orientations
  - Corrosion induced wall thing
  - Geohazard impact
  - Assessment of rehabilitation methods
- Reexamine ASME B31.8 regarding pressurized and unpressurized characterization of dents and gouges.

Project Outcome/ Impact on Pipeline Safety

1. Bastawros, A. -F., “Fundamental Understanding of Pipeline Material Degradation under Interactive Threats of Dents and Corrosion,” Government and Industry Pipeline PHMSA R&D Forum, Washington DC, Oct 31-Nov. 1, 2023.
2. Amir Abdelmawla, Ashraf Bastawros, “Effect of Pre-Accumulated Plastic Strain on Stress Corrosion Cracking and Fatigue Life of Steels; Experiment and Modeling,” International Conference on Fracture, Atlanta, Georgia, June 11 – 16, 2023.
3. A. Abdelmawla, K. Kulkarni and A.F. Bastawros, 2023, Effect of Pre-Accumulated Plastic Strain on Stress Corrosion Cracking and Fatigue Life of Steels; Experiment and Modeling, Conference Proceedings of the Society for Experimental Mechanics Series. Society for Experimental Mechanics Annual Conference and Exposition, Orlando, Florida, June 5 – 8, 2023, (in press).
4. Amir Abdelmawla, Ashraf Bastawros, “Fatigue Damage Model for Predicting the Effect of Pres-straining on the Remaining Fatigue Life of Ti-Alloys,” The Fourth International Conference on Damage Mechanics, Baton Rouge, Louisiana, USA, MAY 15 - 18, 2023.
5. Bastawros, A. –F., (Invited talk). “Corrosion: Interaction between Electrochemistry and Mechanics,” Society of Engineering Sciences Meeting, Texas A&M College Station, October 16-21, 2022.
6. Pratyush Mishra, Denizhan Yavas, Abdullah Alshehri, Pranav Shrotriya, Ashraf Bastawros, Kurt R Hebert, 2021, “Model of vacancy diffusion-assisted intergranular corrosion in low-alloy steel,” Acta Materialia 220: 117348. https://doi.org/10.1016/j.actamat.2021.117348
7. Denizhan Yavas, Thanh Phan, Liming Xiong, Kurt R. Hebert, Ashraf F. Bastawros, 2020, “Mechanical degradation due to vacancies produced by grain boundary corrosion of steel,” Acta Materialia 200, 471-480. https://doi.org/10.1016/j.actamat.2020.08.080
8. Bastawros, A. -F., “Fundamental Understanding of Pipeline Material Degradation under Interactive Threats of Dents and Corrosion,” Government and Industry Pipeline R&D Forum, Washington DC, February 19-20, 2020.
9. Pratyush Mishra, Denizhan Yavas, Abdullah Ashehri, Ashraf Bastawros, Pranav Shrotriya, Kurt Heber “Mechanism for Propagation of Intergranular Corrosion in Pipeline Steel,” 236th ECS Meeting, Atlanta GA Oct. 13-17, 2019.
10. Denizhan Yavas, Thanh Phan, Liming Xiong, Kurt Hebert, Ashraf Bastawros, 2019, “Atomistic study of grain boundary degradation under intergranular electrochemical attack,” Society of Engineering Sciences Meeting, St Louis MO, October 13-15, 2019.

Thank You!

Presentation and final Report are posted on project public Page

https://primis.phmsa.dot.gov/matrix/PrjHome.rdm?prj=838

Questions and comments for PI:

Ashraf Bastawros bastaw@iastate.edu